

# ***M3 PPR Battery Development***

**David Petrushenko<sup>1,3</sup>, Paul Coman<sup>3</sup>, Jesus Trillo<sup>1</sup>, Jacob Darst<sup>1</sup>, Ralph White<sup>3</sup> and Eric Darcy<sup>1</sup>**

**Jacob L. Moyar<sup>2</sup>, John R. Izzo<sup>2</sup>, Thomas E. Adams<sup>2</sup>, and Joe H. Fontaine<sup>2</sup>**

**<sup>1</sup>NASA-Johnson Space Center**

**<sup>2</sup>Naval Sea Systems Command Warfare Centers (NSWC, NUWC)**

**<sup>3</sup>Department of Chemical Engineering, University of South Carolina**

**NASA Aerospace Battery Workshop**

**15-17 November 2022**

# Presentation Outline

- Motivation and Background
  - Modeling-Informed Design Predictions (COMSOL)
    - Heat Sink Comparisons
    - Electrical Bus Plate Comparisons
    - Bus Bar Comparisons
    - Modeling Thermal Runaway and Trigger Cell Locations
  - Battery Design Details
    - Cell Preparation
    - Battery Assembly Details
  - Thermal Runaway Results
    - Thermal Runaway Test
    - Post-Test DPA Results

# Motivation for Development of “M3”

- Design and test a high-performance battery pack with application for remote operated vehicle application to pass Passively Propagation Resistant (PPR) thermal runaway testing
- Battery design details:
  - 134P (parallel) virtual cell using commercial 18650 cell
  - 3S (series) axial stack of the 134P-virtual cells protected by ceramic-reinforced blast plate
  - 12 strategically placed ISCD trigger cells to produce single-point cell failures simulate failure of individual cell
- Survive 12 individual TR events without propagation and no blast plate perforations
- Meet temperature and mass operational requirements and fit within prescribed allowable volume

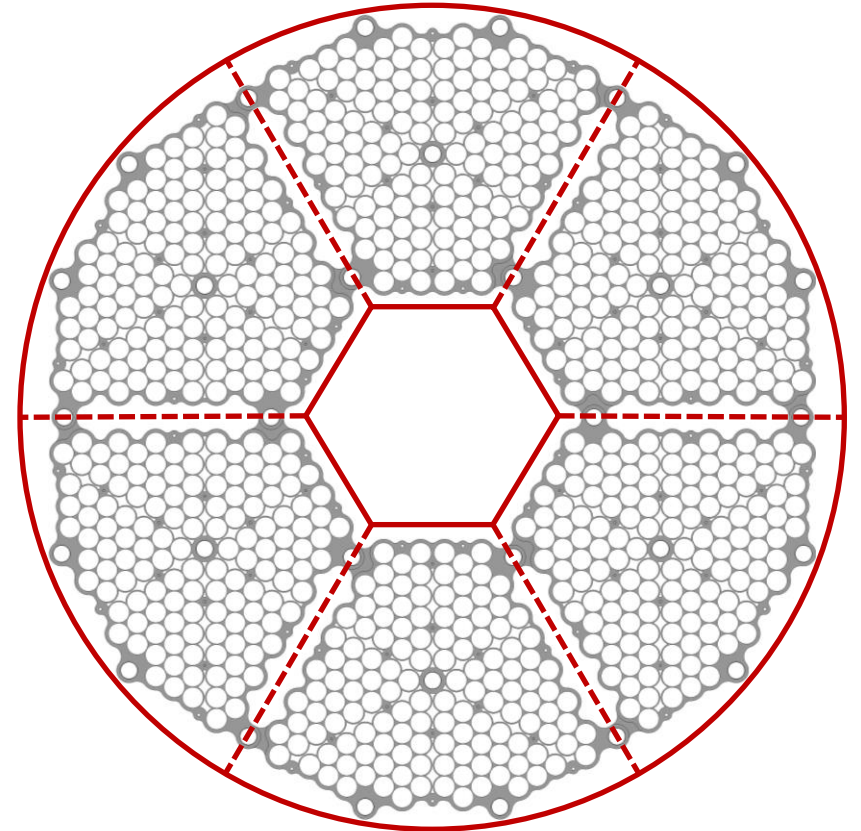
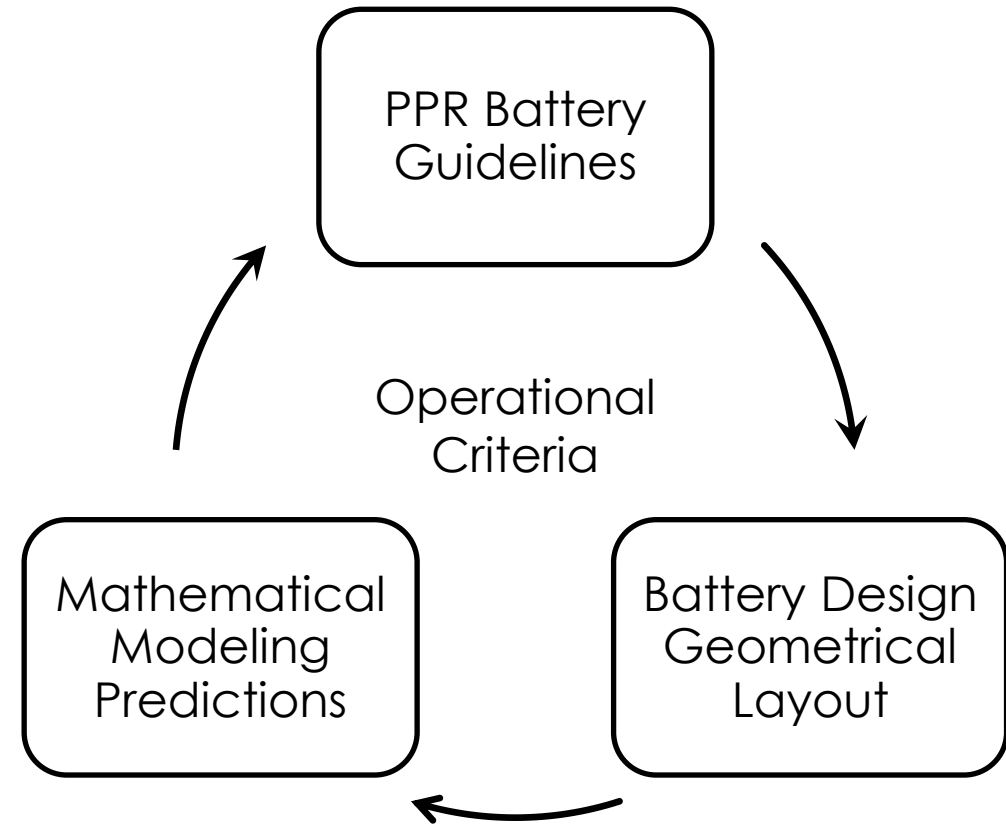


**Figure:** Battery spatial constraints defined in red.

# Criteria for TR Propagation Resistant Batteries

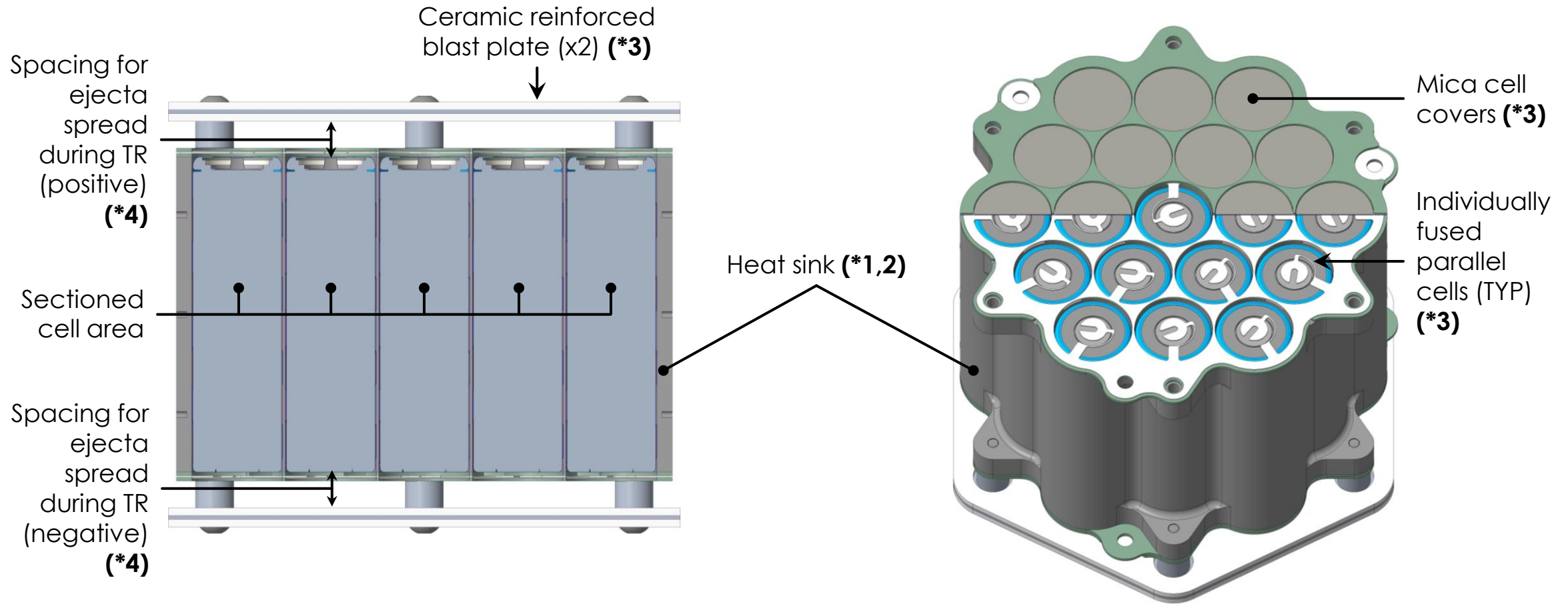
## Guidelines for PPR Batteries:

1. Reduce the risk of cell can side wall breaches (sidewall rupture)
2. Provide adequate cell spacing and heat rejection
3. Individually fuse parallel cells
4. Protect the adjacent cells from the hot TR ejecta
5. Prevent flames and sparks from exiting the battery



**Reference:** Darcy, E. C., Jacob, D., Walker, W., Finegan, D. P. & Shearing, P. Driving Design Factors for Safe, High-Power Batteries for Space Applications. in Advanced Automotive Battery Conference (2018).

# PPR Battery Guideline Design Examples



**Note:** an asterisk followed by a number (e.g. \*1) indicates the PPR Battery Guideline the feature correlates to. Guideline 5 (battery enclosure) example is not shown for clarity.

# SUMMARY OF MODELING RESULTS

# Cell Heating Profiles vs Depth of Discharge

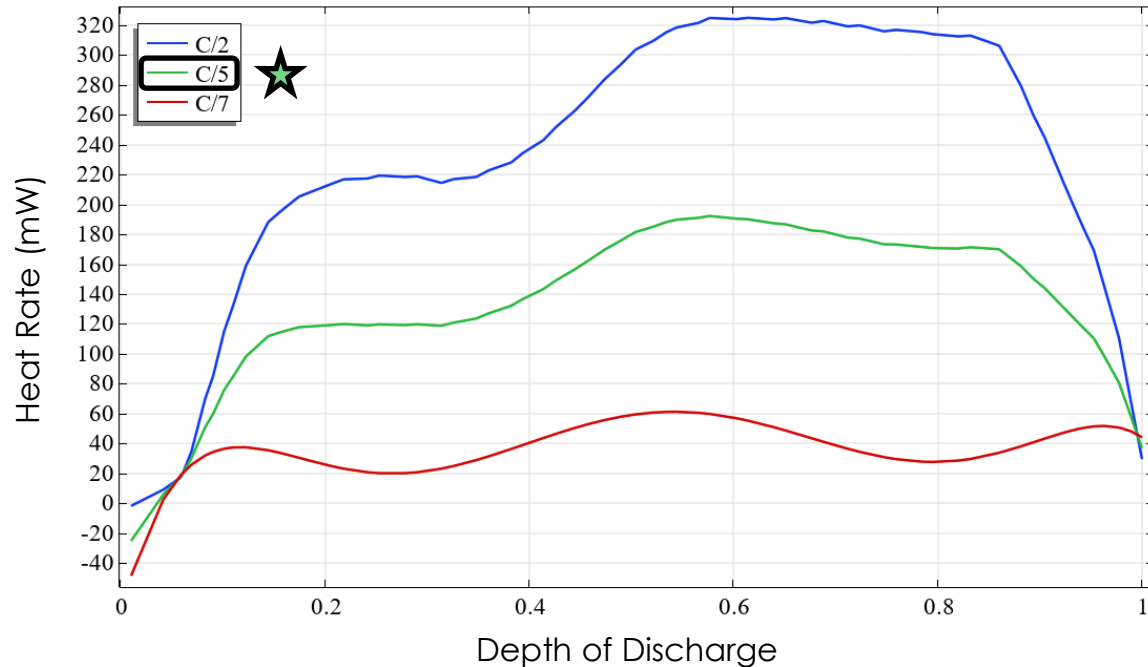


**Figure:** Cell heat generation rate during charging at 40 °C as a function of Depth of Discharge (DoD). Average values used for thermal modeling: C/2:  $\dot{Q}_{avg} = 225.9$  mW, C/5:  $\dot{Q}_{avg} = 131.8$  mW, C/7:  $\dot{Q}_{avg} = 37.7$  mW.

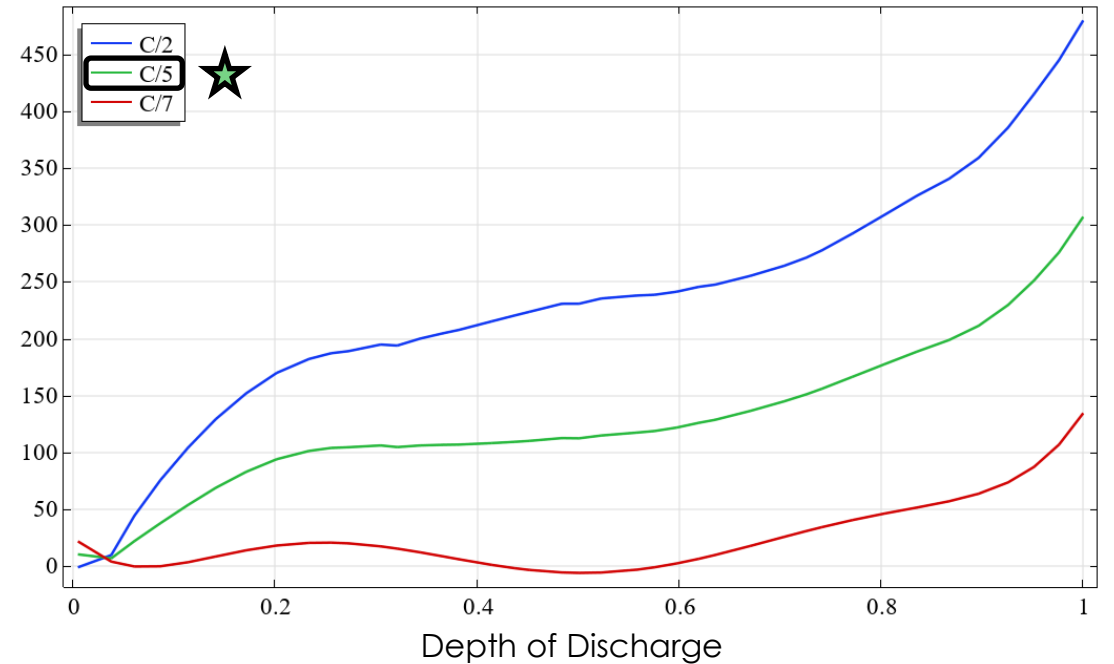


**Figure:** Cell heat generation rate during discharge at 20 °C as a function of Depth of Discharge (DoD). Average values used for thermal modeling: C/2:  $\dot{Q}_{avg} = 230.9$  mW, C/5:  $\dot{Q}_{avg} = 127.2$  mW, C/7:  $\dot{Q}_{avg} = 23.5$  mW.

# Heat Sink Thermal Modeling – Design A

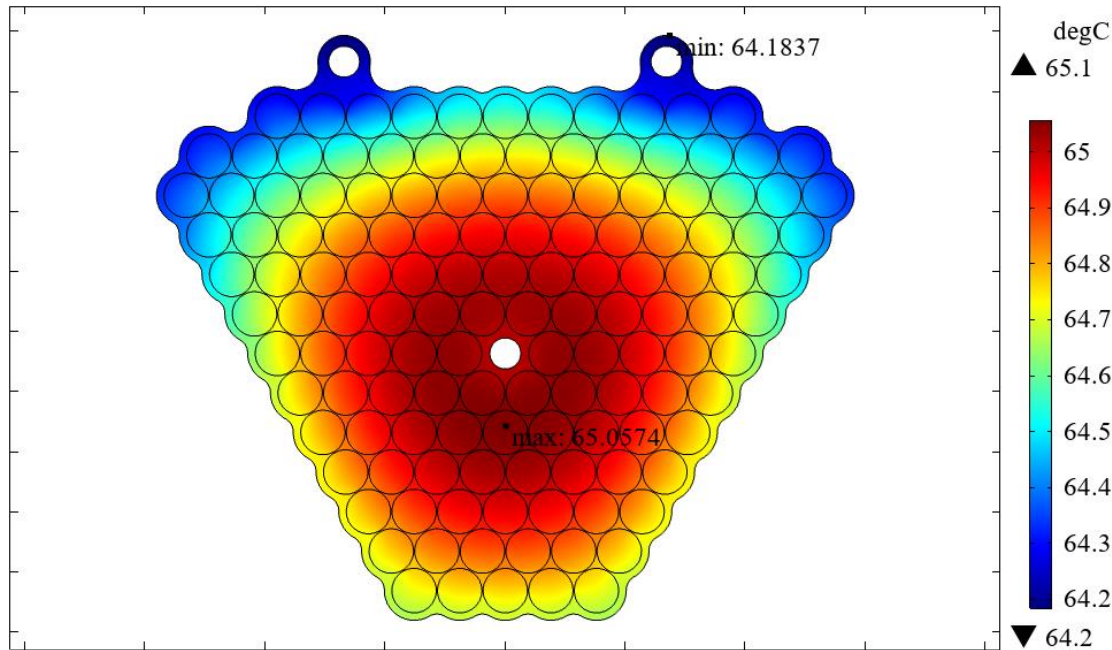


**Figure:** Temperature generated during **charging (C/5 at 5hrs)** with an ambient temperature of 40 °C. This heat sink design features a close-packed grouping spacing cells at 0.020" apart providing a baseline for comparison.

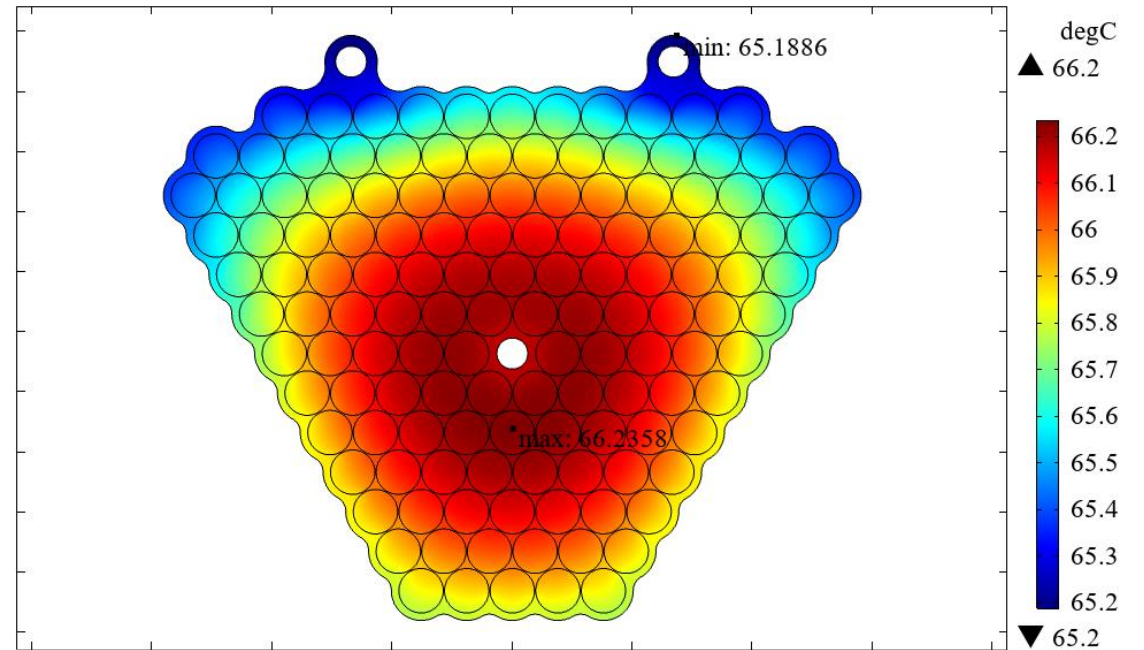


**Figure:** Temperature generated during **discharging (C/5 at 5hrs)** with an ambient temperature of 40 °C. This heat sink design features a close-packed grouping spacing cells at 0.020" apart providing a baseline for comparison.

# Heat Sink Thermal Modeling – Design B

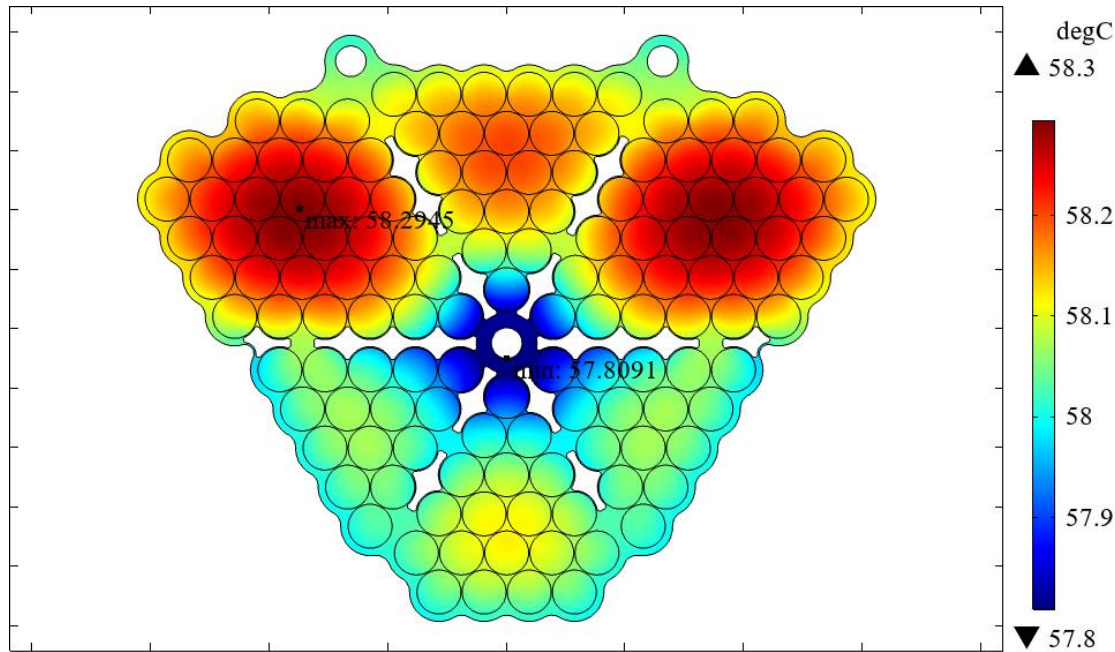


**Figure:** Temperature generated during **charging (C/5, at 5hrs)** with an ambient temperature of 40 °C. This heat sink design features a triangular cell-grouping with air gaps between neighboring cell groups. Temperature **drop of 6.8°C** observed compared to Design A (~27% difference).

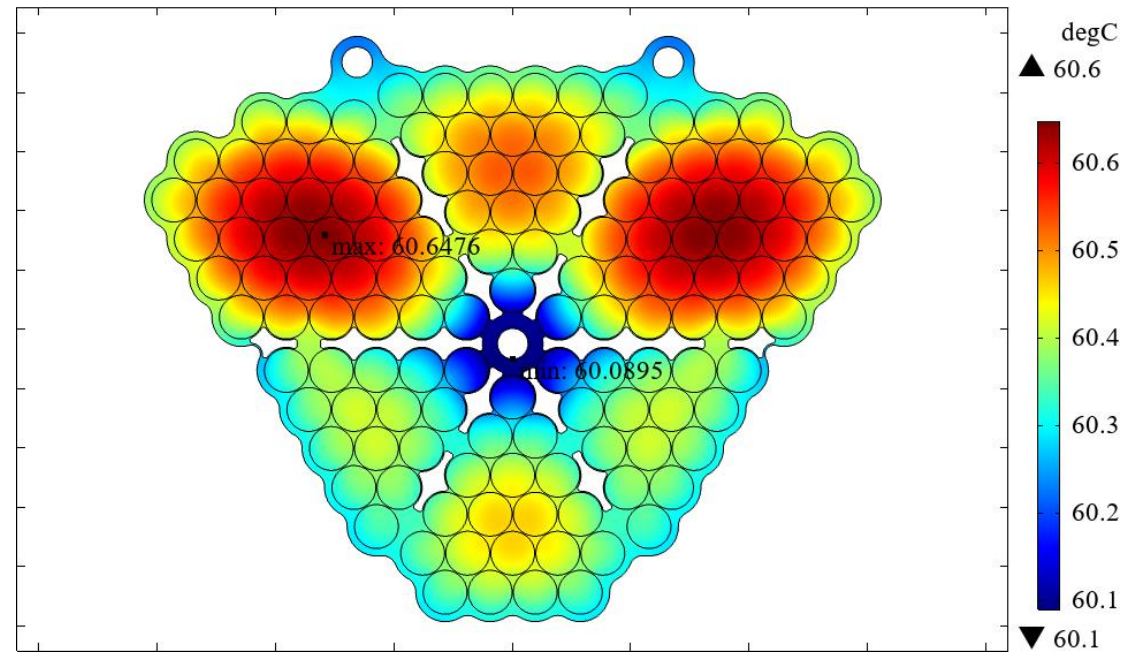


**Figure:** Temperature generated during **charging (C/5, at 5hrs)** with an ambient temperature of 40 °C. This heat sink design features a triangular cell-grouping with air gaps between neighboring cell groups. Temperature **drop of 5.6°C** observed compared to Design A (~21% difference).

# Heat Sink Thermal Modeling – Design C

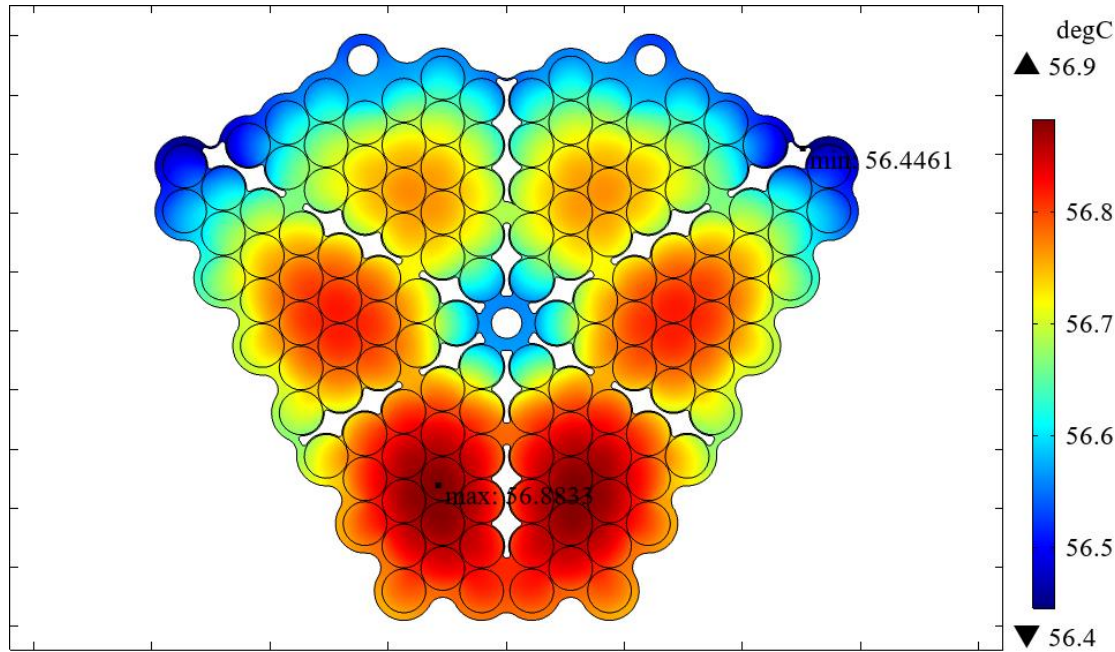


**Figure:** Temperature generated during **charging (C/5, at 5hrs)** with an ambient temperature of 40 °C. Heat sink Design C features a different triangular cell-grouping compared to Design B. Temperature **drop of 8.2°C** observed compared to Design A (~33% difference).

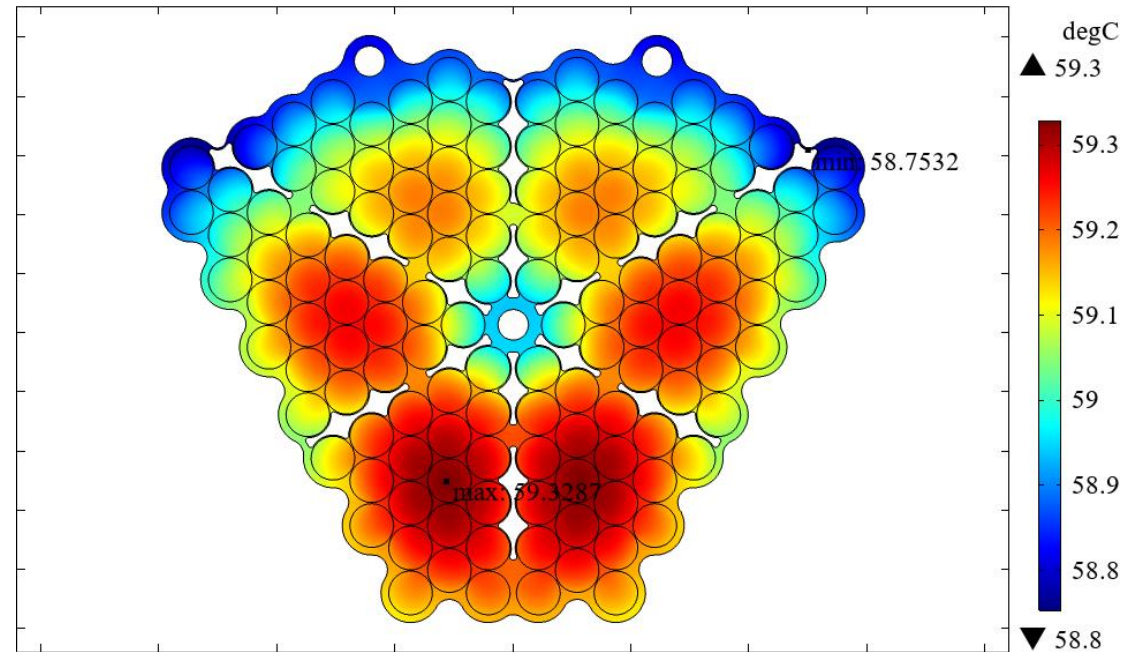


**Figure:** Temperature generated during **charging (C/5, at 5hrs)** with an ambient temperature of 40 °C. Heat sink Design C features a different triangular cell-grouping compared to Design B. Temperature **drop of 6.9°C** observed compared to Design A (~26% difference).

# Heat Sink Thermal Modeling – Design D

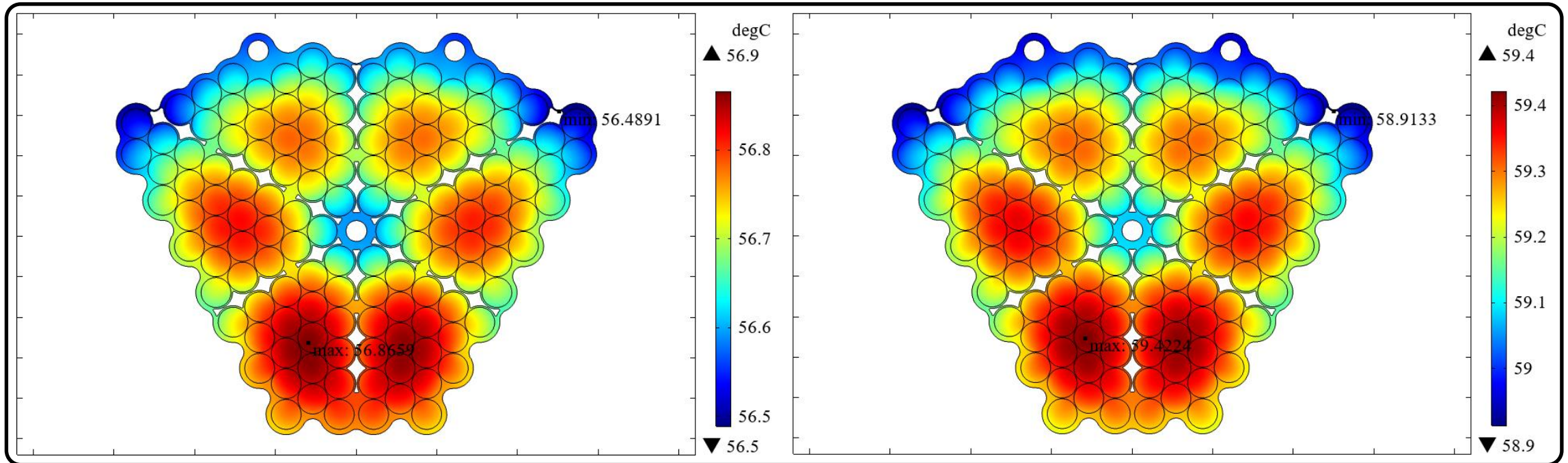


**Figure:** Temperature generated during **charging (C/5, at 5hrs)** with an ambient temperature of 40 °C. Design D features slightly thicker aluminum in the internal “air gap” areas compared to Design C. Temperature **drop of 8.2°C** observed compared to Design A (~33% difference).

**Figure:** Temperature generated during **charging (C/5, at 5hrs)** with an ambient temperature of 40 °C. Design D features slightly thicker aluminum in the internal “air gap” areas compared to Design C. Temperature **drop of 6.8°C** observed compared to Design A (~26% difference).

# Heat Sink Thermal Modeling – Summary

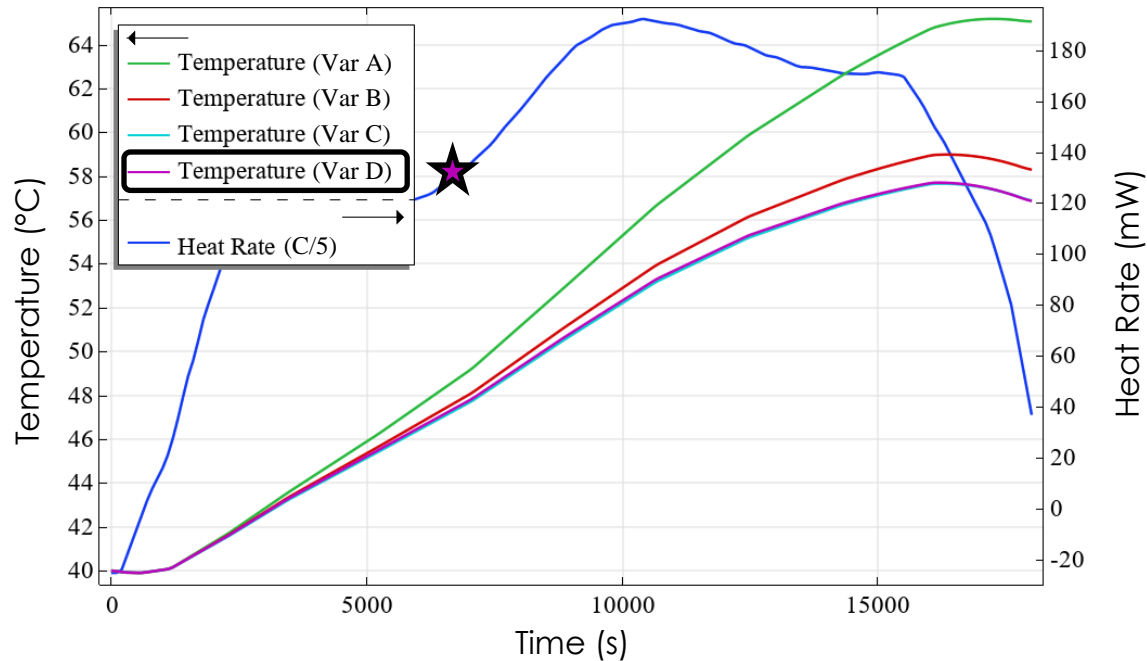


**Figure:** Maximum temperature predictions during **charging (C/5)** as a function of time (5 hr limit) in heat sink Designs A-D. Charging simulated at an ambient temperature of 40 °C. Note temperature differences with added air gap between cell groupings (Designs B-D).

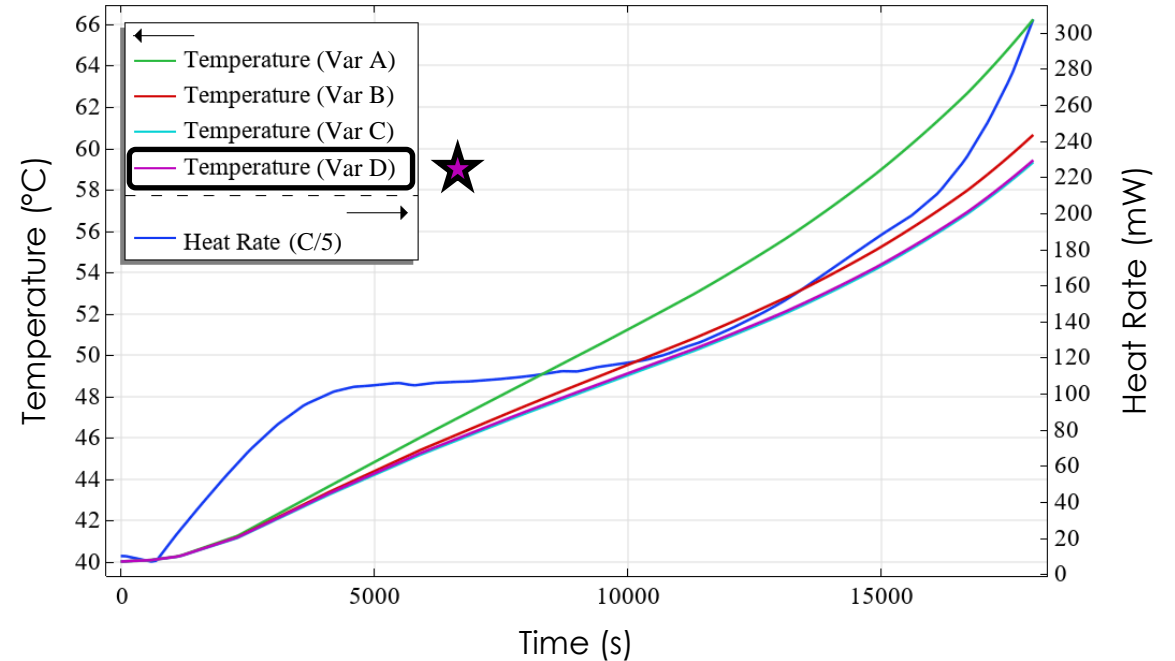
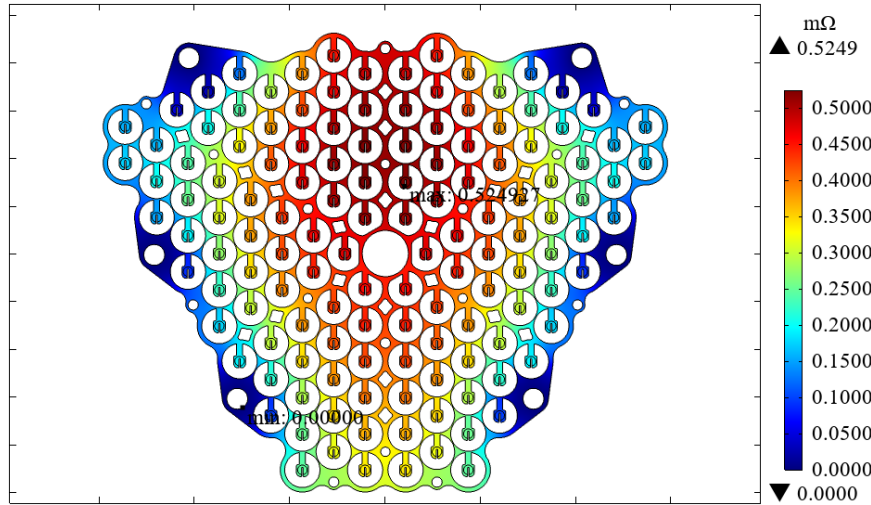


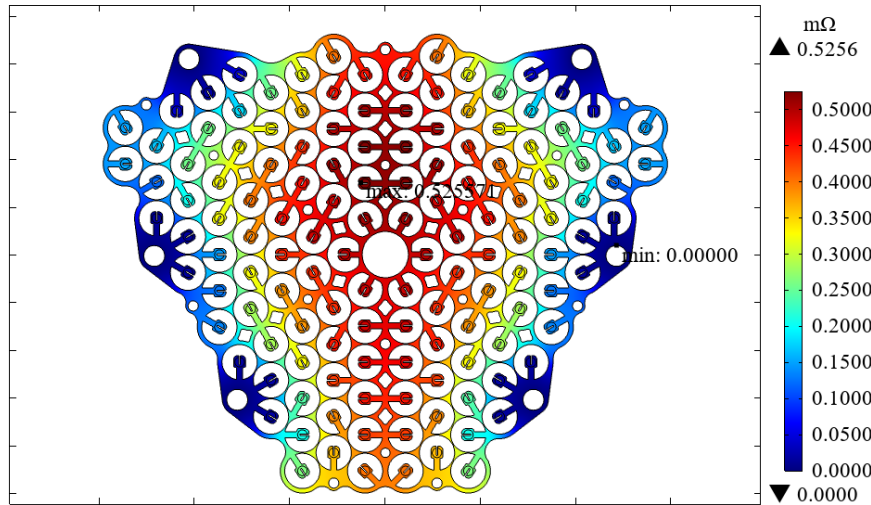
**Figure:** Maximum temperature predictions during **discharging (C/5)** as a function of time (5 hr limit) in heat sink Designs A-D. Charging simulated at an ambient temperature of 40 °C. Note temperature differences with added air gap between cell groupings (Designs B-D).

# Bus Plate Electrical Resistance Modeling

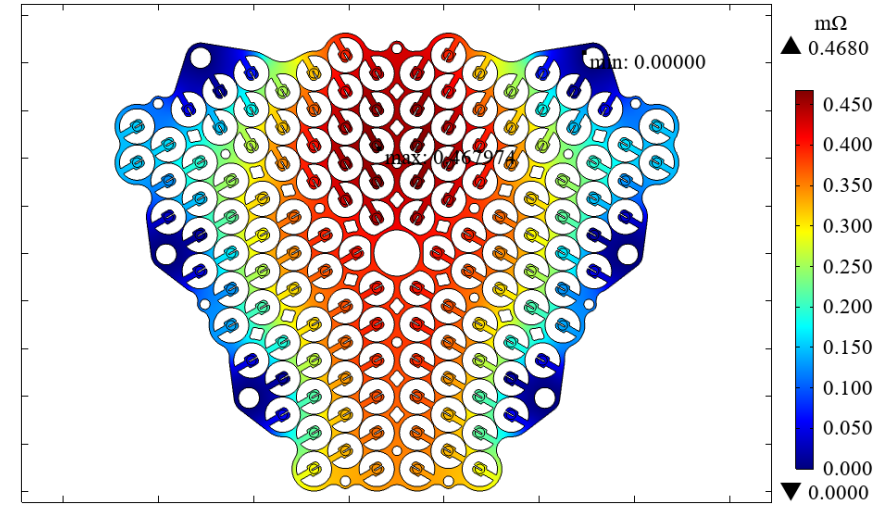
► Positive bus plate **Design A**. Max predicted resistance: **0.52 mΩ**, a **15%** rise compared to Design D. (1.5A per cell, 200A total current, Nickel 200).



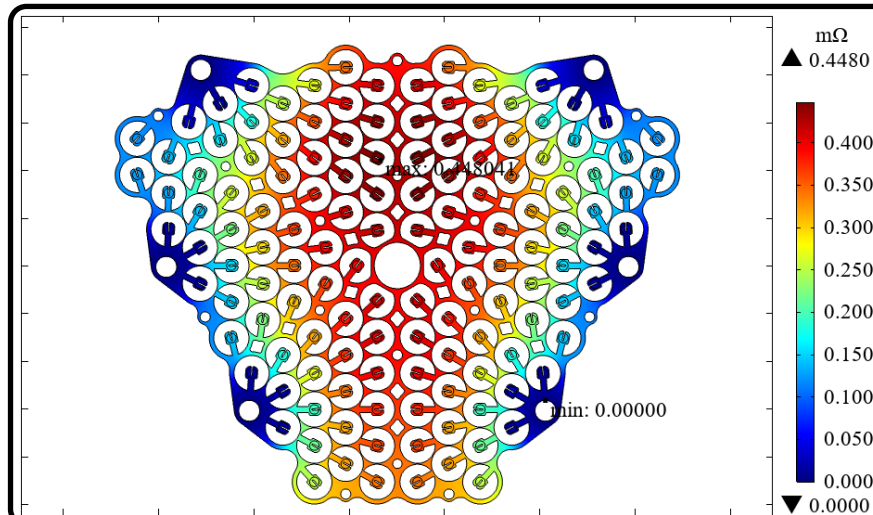
► Positive bus plate **Design C**. Max predicted resistance: **0.53 mΩ**, a **15%** rise compared to Design D. (1.5A per cell, 200A total current, Nickel 200).



◀ Positive bus plate **Design B**. Max predicted resistance: **0.47 mΩ**, a **4.3%** rise compared to Design D. (1.5A per cell, 200A total current, Nickel 200).

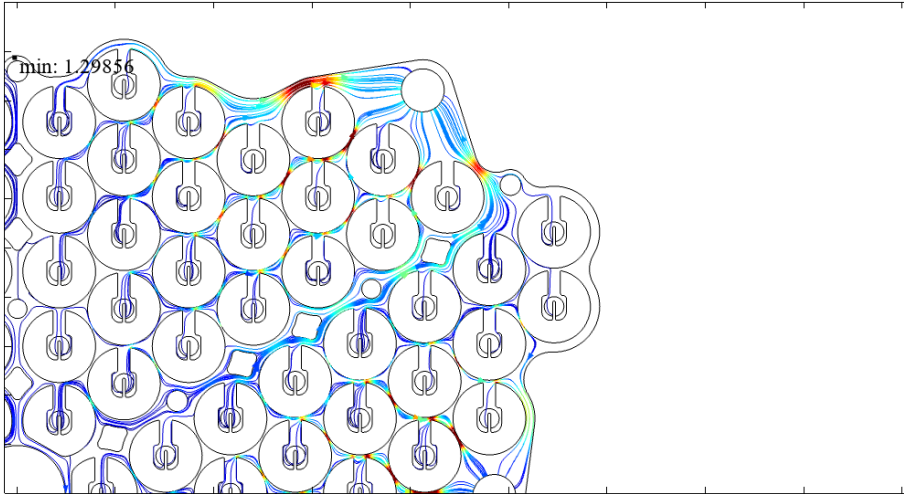


◀ Positive bus plate **Design D**. Max predicted resistance: **0.45 mΩ**, lowest resistance of four designs. (1.5A per cell, 200A total current, Nickel 200).

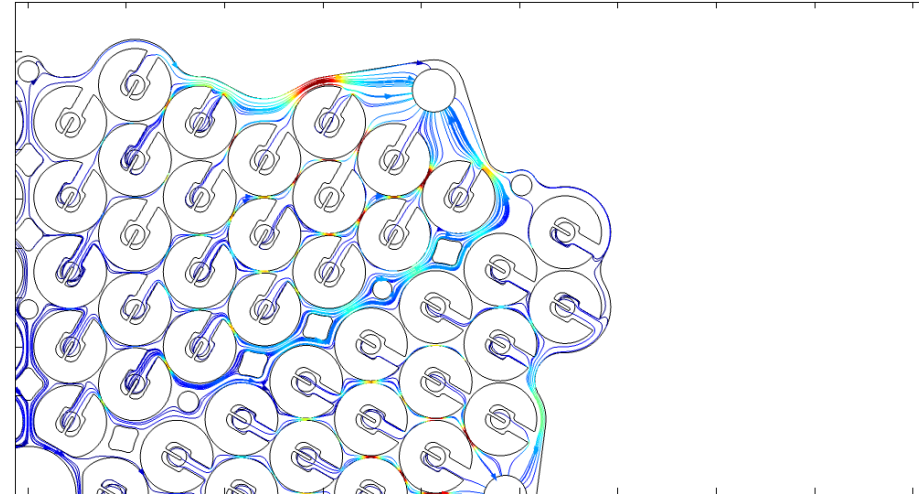


# Bus Plate Electrical Resistance Modeling (cont).

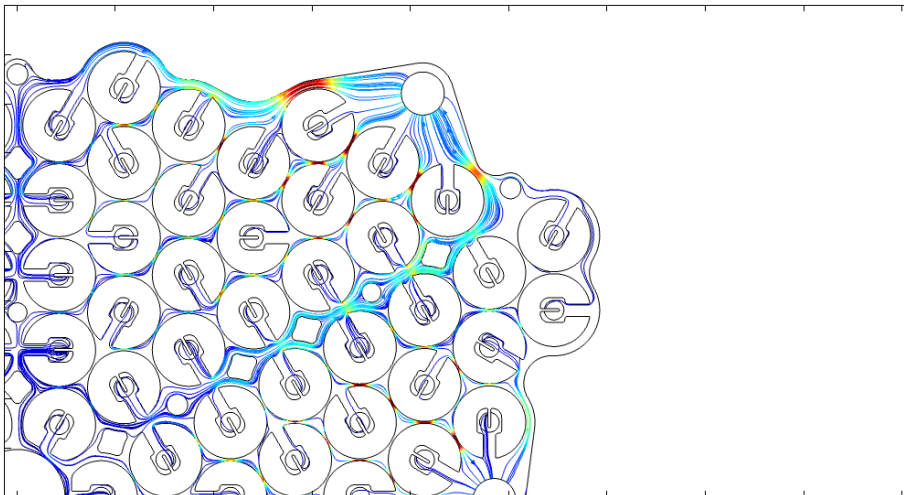
► Positive bus plate **Design A** current density from terminal ring (upper right, 1.5A per cell, 200A total current, Nickel 200).



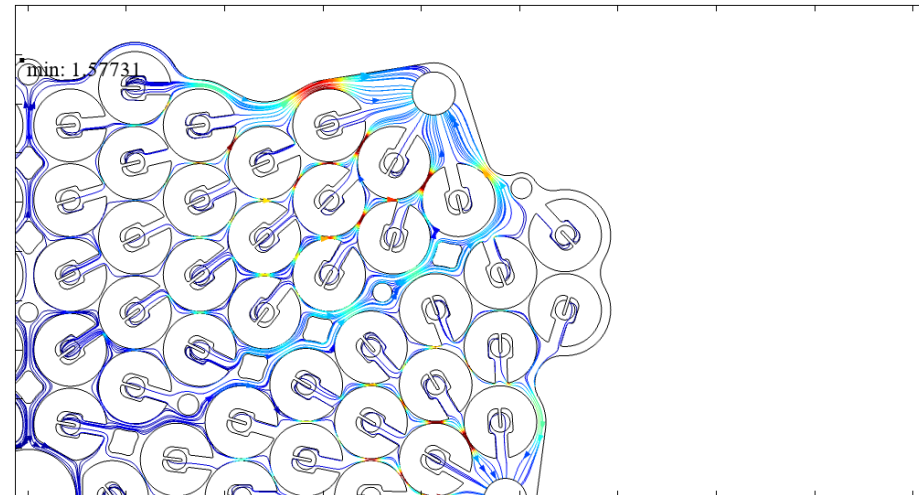
◄ Positive bus plate **Design B** current density from terminal ring (upper right, 1.5A per cell, 200A total current, Nickel 200).



► Positive bus plate **Design C** current density from terminal ring (upper right, 1.5A per cell, 200A total current, Nickel 200).

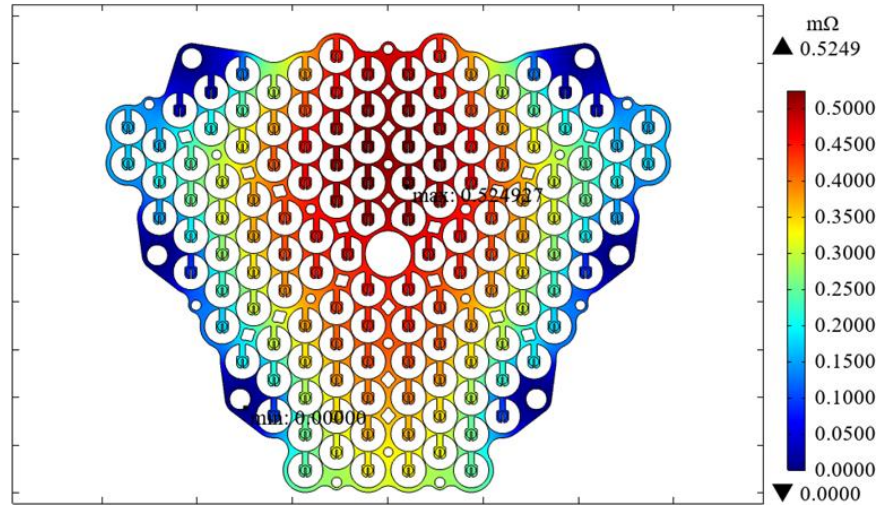


◄ Positive bus plate **Design D** current density from terminal ring (upper right, 1.5A per cell, 200A total current, Nickel 200).

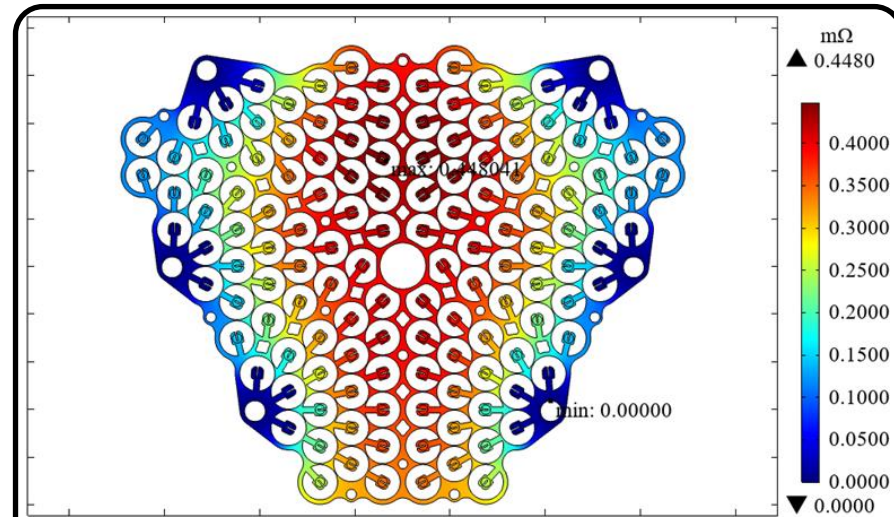
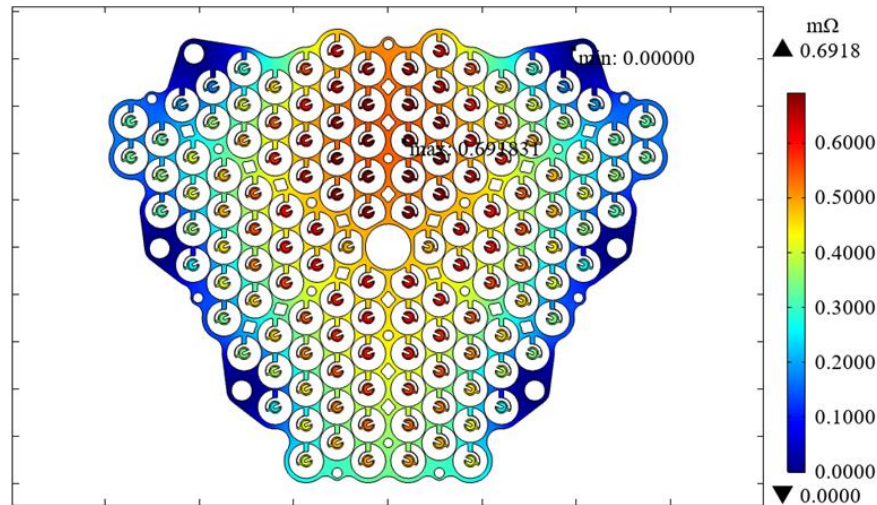


# Bus Plate Electrical Resistance Modeling (cont).

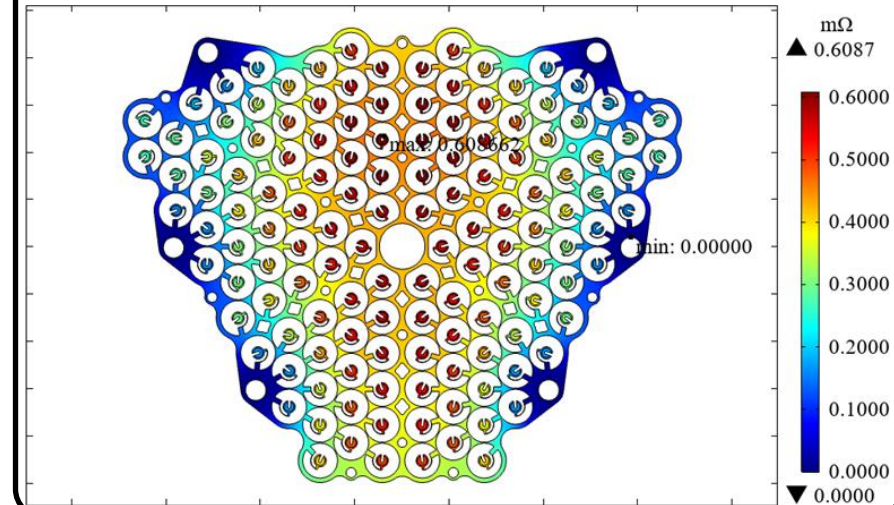
► Positive bus plate **Design A**.  
Max predicted resistance: **0.52 mΩ**, a 15% rise compared to Design D. (1.5A per cell, 200A total current, Nickel 200).



► Negative bus plate **Design A**.  
Max predicted resistance: **0.69 mΩ**, a 12% rise compared to Design D. (1.5A per cell, 200A total current, Nickel 200).



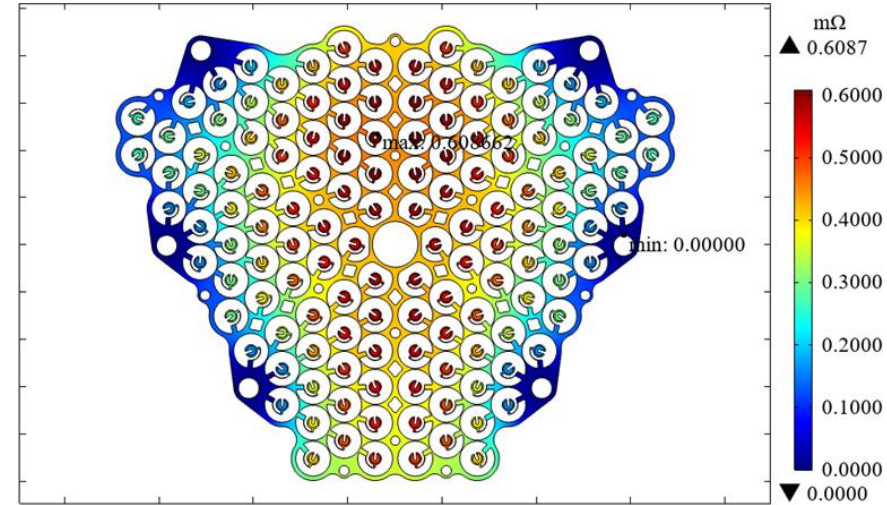
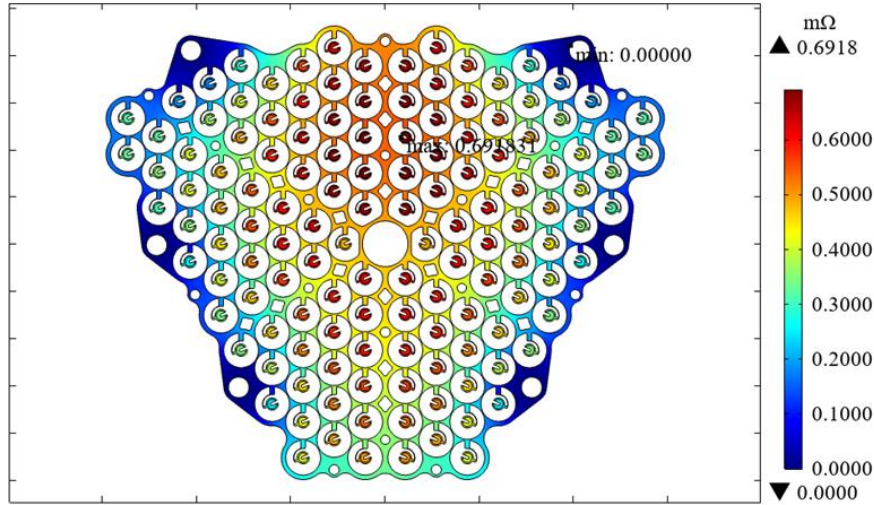
◀ Positive bus plate **Design D**.  
Max predicted resistance: **0.45 mΩ**. (1.5A per cell, 200A total current, Nickel 200).



◀ Negative bus plate **Design D**.  
Max predicted resistance: **0.61 mΩ**. (1.5A per cell, 200A total current, Nickel 200).

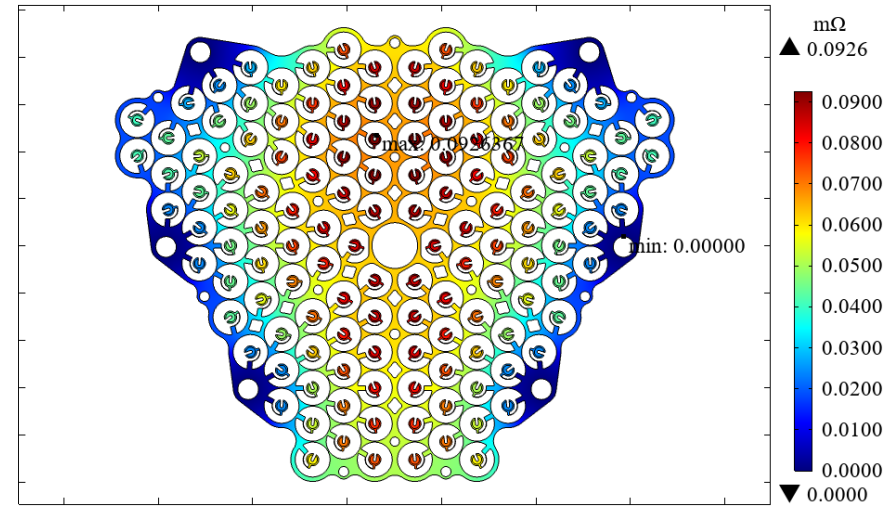
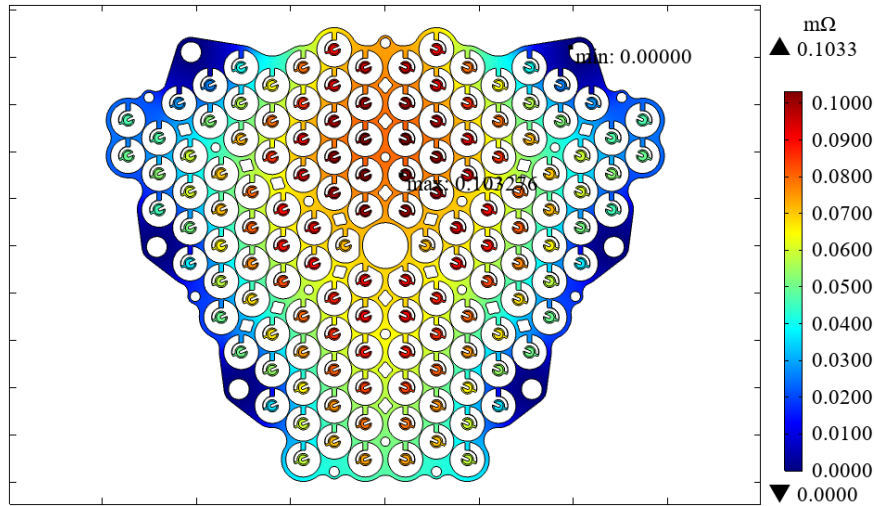
# Negative Bus Plate Material Comparisons

► Negative bus plate **Design A**. Max predicted resistance: **0.69 mΩ**, a **12%** rise compared to Design D. (1.5A per cell, 200A total current, Nickel 200, 0.010" thick).



◀ Negative bus plate **Design D**. Max predicted resistance: **0.61 mΩ**. (1.5A per cell, 200A total current, Nickel 200, 0.010" thick).

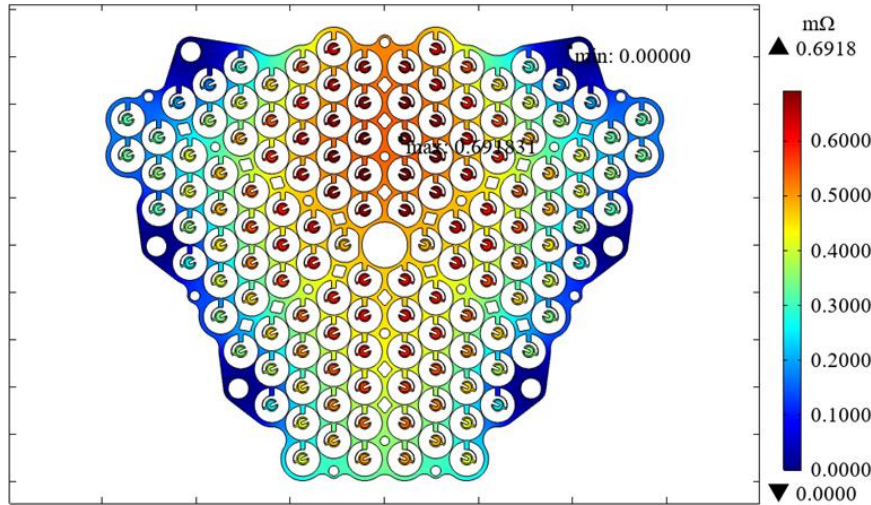
► Negative bus plate **Design A**. Max predicted resistance: **0.10 mΩ**, a **10%** rise compared to Design D. (1.5A per cell, 200A total current, Copper 101, 0.010" thick).



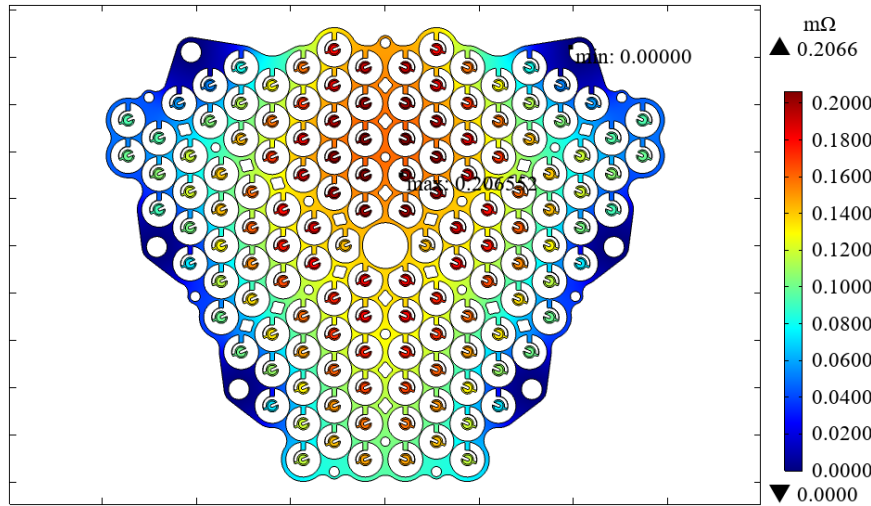
◀ Negative bus plate **Design D**. Max predicted resistance: **0.09 mΩ**, an **85%** drop compared to Nickel 201. (1.5A per cell, 200A total current, Copper 101, 0.010" thick).

# Negative Bus Plate Material Comparisons (cont.)

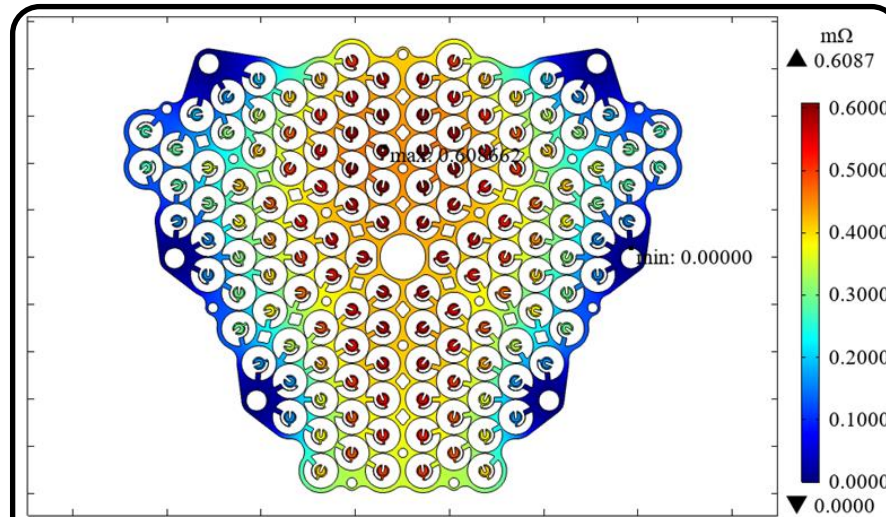
► Negative bus plate **Design A**. Max predicted resistance: **0.69 mΩ**, a **12%** rise compared to Design D. (1.5A per cell, 200A total current, Nickel 200, 0.010" thick).



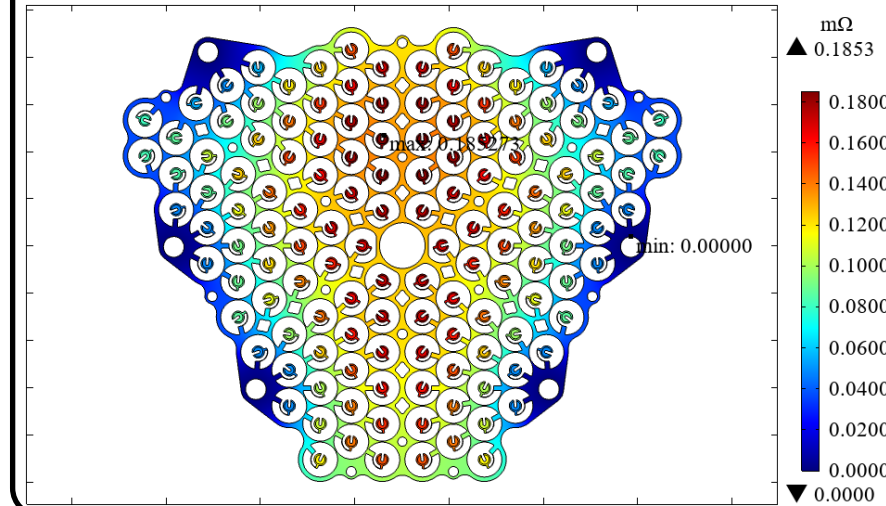
► Negative bus plate **Design A**. Max predicted resistance: **0.21 mΩ**, a **10%** rise compared to Design D. (1.5A per cell, 200A total current, Copper 101, 0.005" thick).



◄ Negative bus plate **Design D**. Max predicted resistance: **0.61 mΩ**. (1.5A per cell, 200A total current, Nickel 200, 0.010" thick).

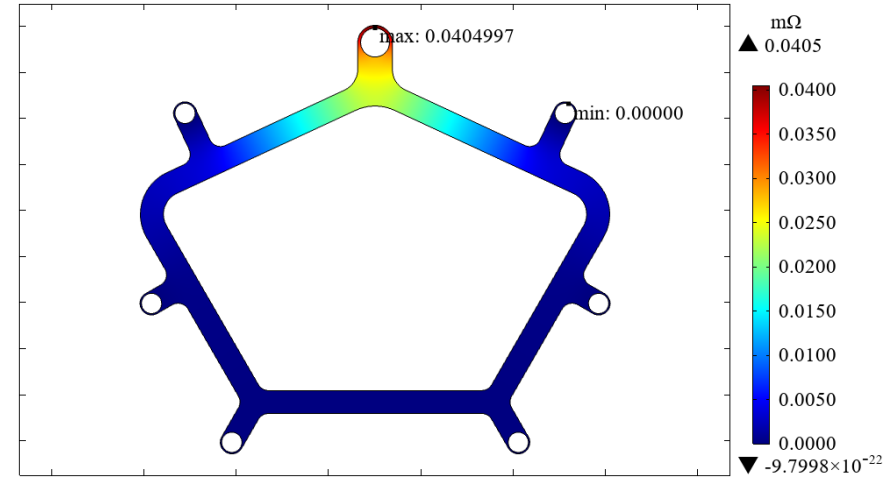
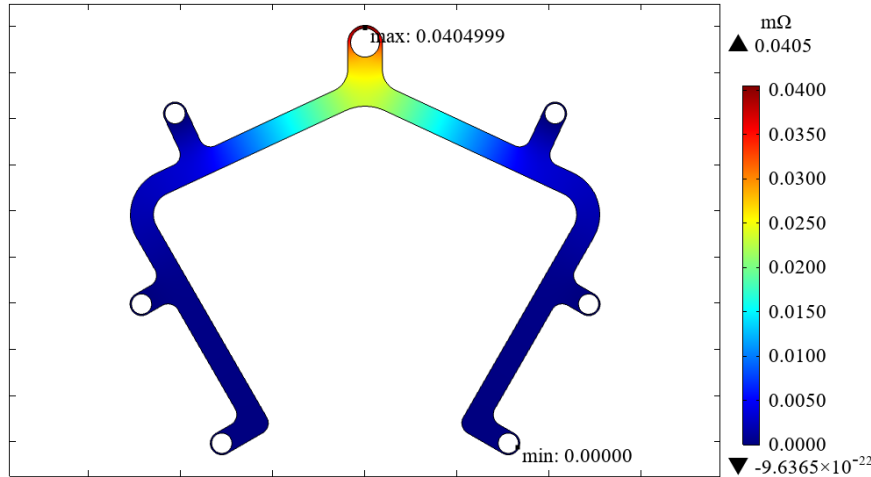


◄ Negative bus plate **Design D**. Max predicted resistance: **0.19 mΩ**, a **70%** drop compared to Nickel 201. (1.5A per cell, 200A total current, Copper 101, 0.005" thick).



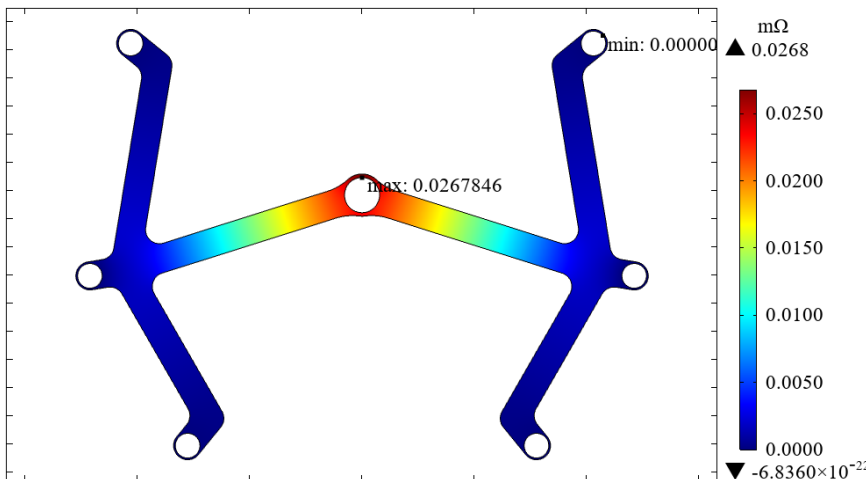
# Bus Bar Electrical Resistance Modeling

► Bus bar **Design A**. Max predicted resistance: **0.041 mΩ**, a **34%** rise compared to Design C. (18A total current, 6061 Aluminum, 0.1875" thick).



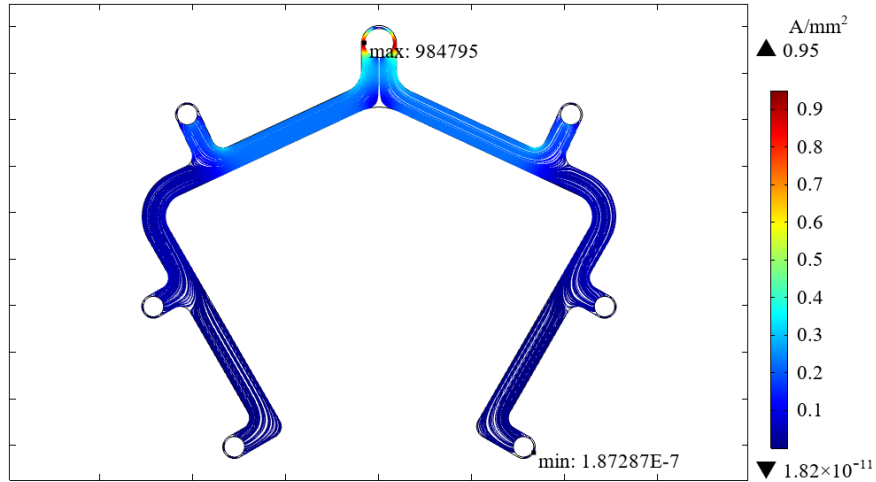
◄ Bus bar **Design A**. Max predicted resistance: **0.041 mΩ**, a **34%** rise compared to Design C. (18A total current, 6061 Aluminum, 0.1875" thick).

► Bus bar **Design C**. Max predicted resistance: **0.027 mΩ**, lowest resistance of three designs. (18A total current, 6061 Aluminum, 0.1875" thick).

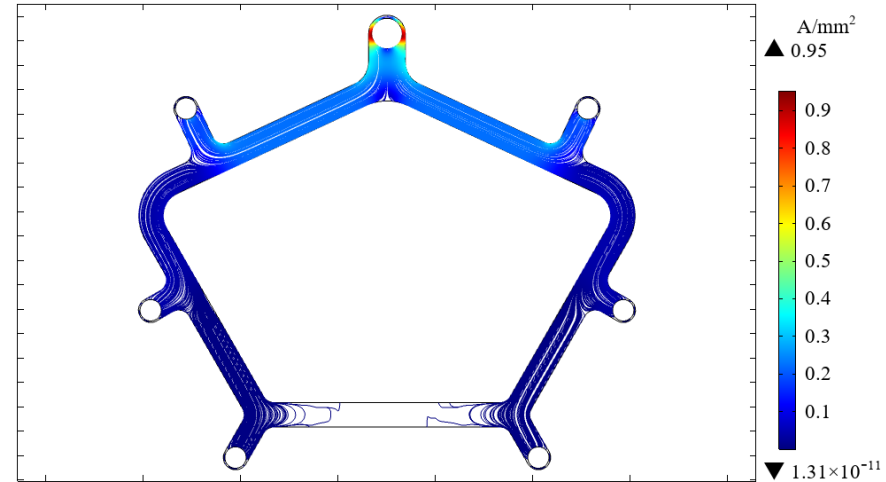


# Bus Bar Electrical Resistance Modeling (cont.)

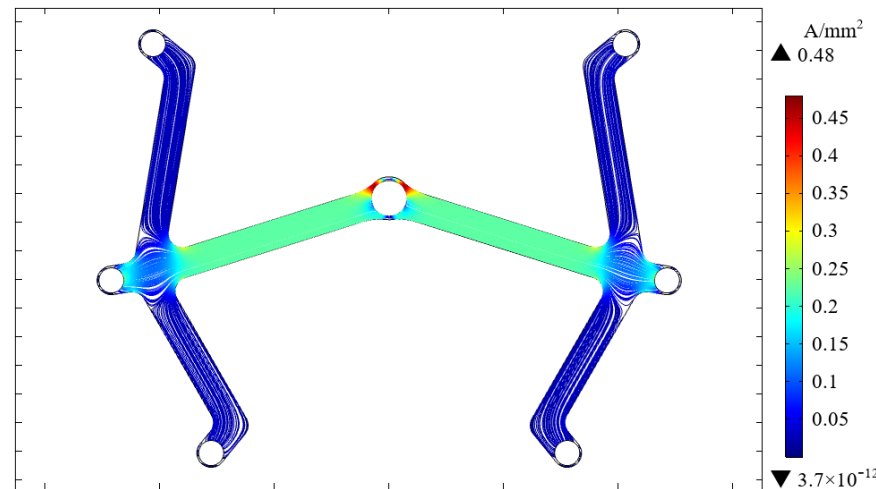
► Bus bar **Design A** current density from terminal lug. (18A total current, 6061 Aluminum, 0.1875" thick).



► Bus bar **Design B** current density from terminal lug. (18A total current, 6061 Aluminum, 0.1875" thick).



► Bus bar **Design B** current density from terminal lug. (18A total current, 6061 Aluminum, 0.1875" thick).



# TR Modeling and Trigger Cell Selection

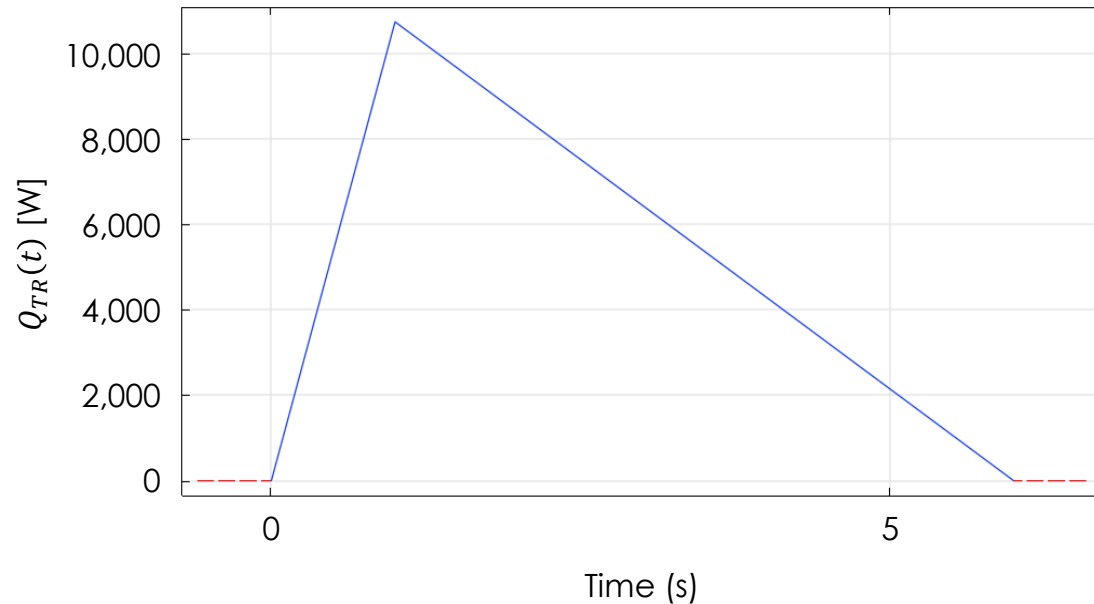


**Figure:** Function extracted from individual cell testing using NASA's Fractional Thermal Runaway Calorimeter (FTRC) representing the thermal heat generated during thermal runaway (TR). This function models the heat transferred from the cell to the cell chamber which measures the heat output from the cell can during the TR event.

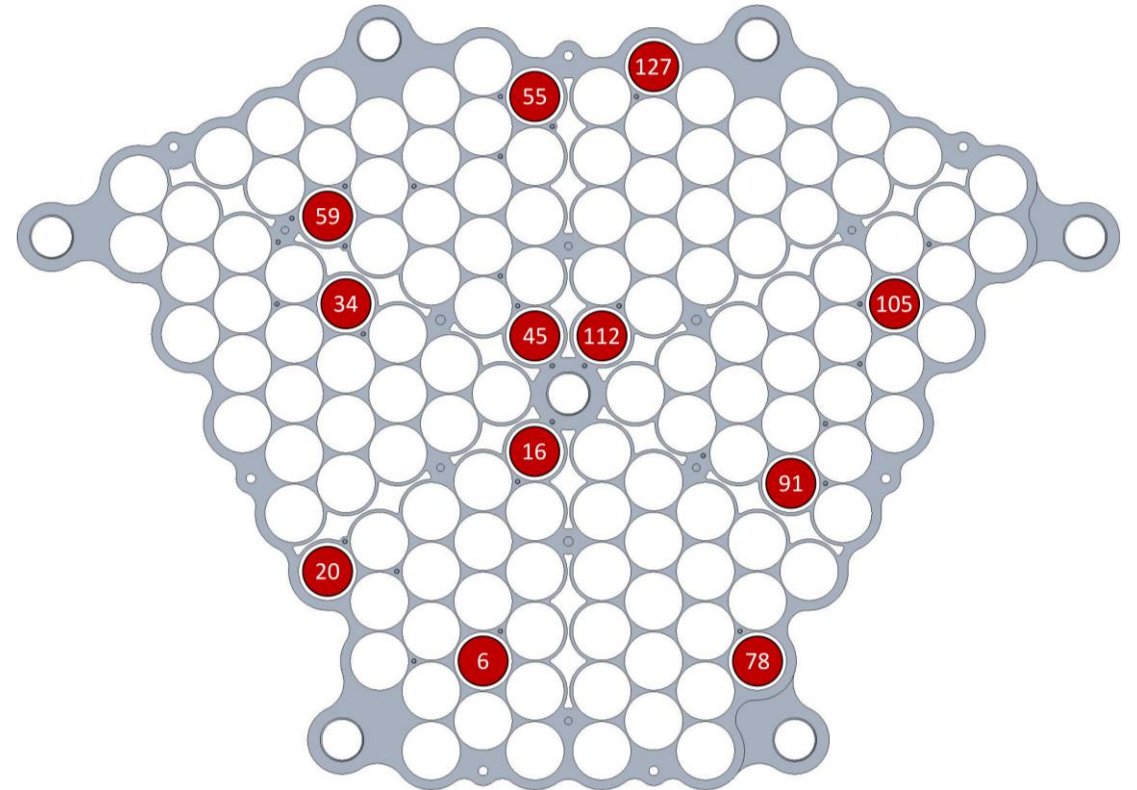
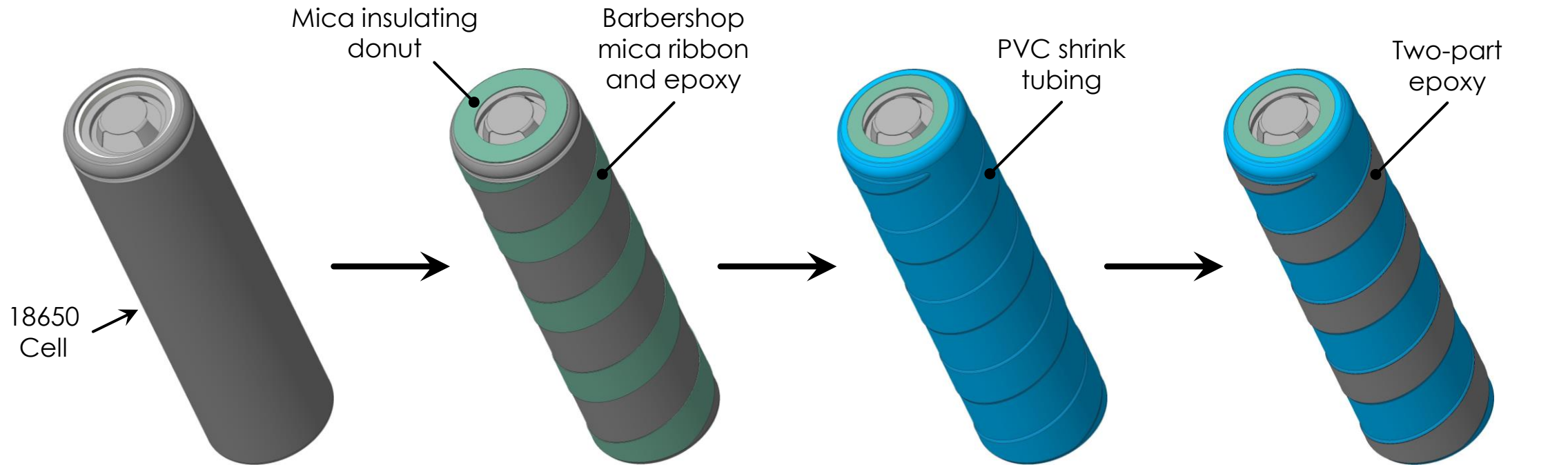


**Figure:** Twelve cell locations for installation of trigger cells guided by thermal runaway modeling.

# BATTERY DESIGN AND ASSEMBLY DETAILS

# Cell Preparation Procedure



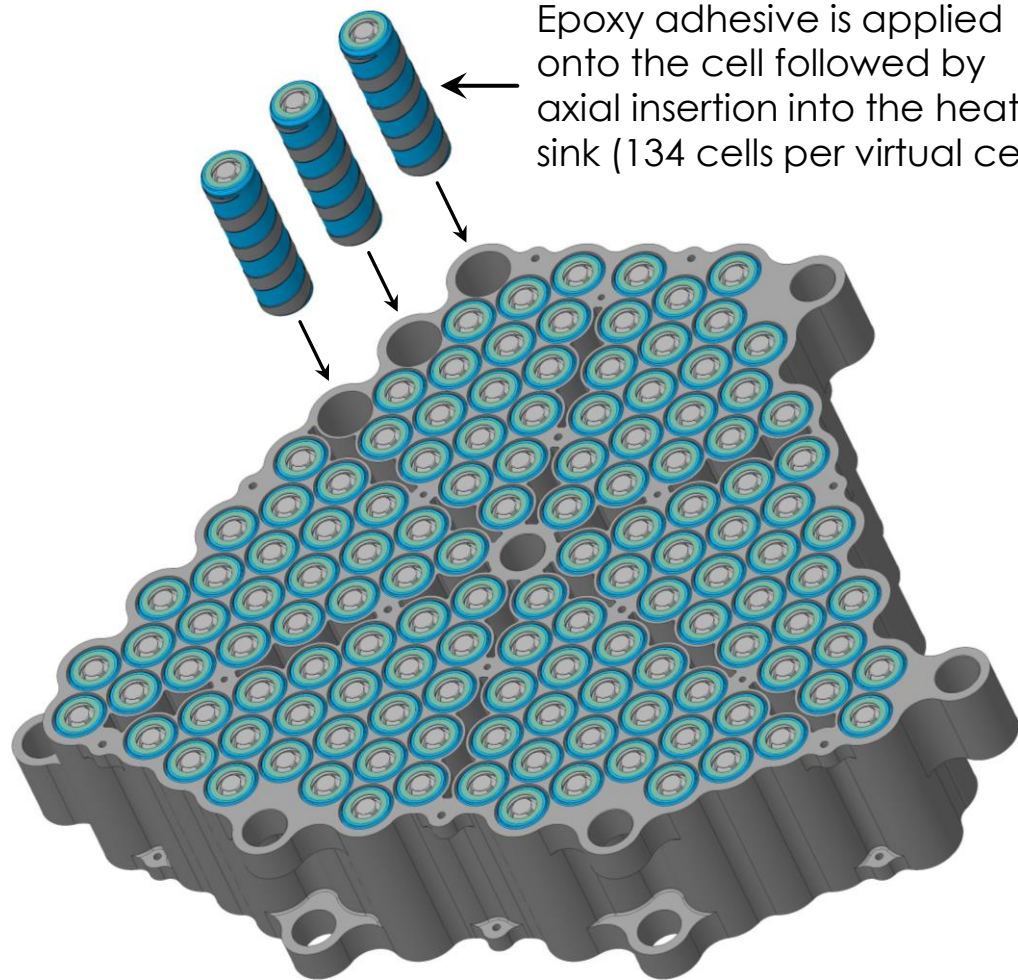
**Step 1:** Manufacturer installed shrink tubing removed with particular care taken not to scratch or score cell can.

**Step 2:** Application of mica ribbon bonded with adhesive. Installation of insulating donut.

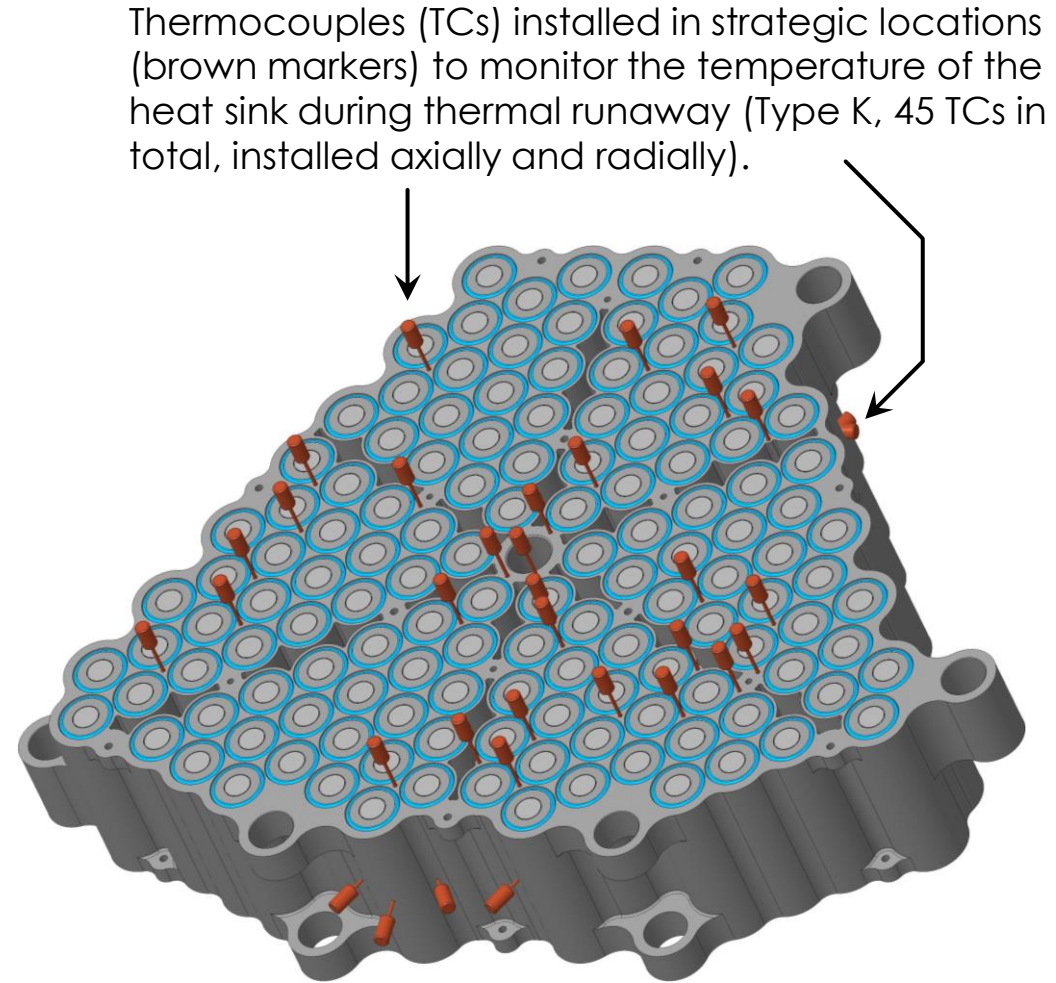
**Step 3:** Installation of PVC-shrink tubing immediately following application of epoxy/mica ribbon to provide clamping.

**Step 4:** Application of adhesive on mica ribbon spiral for installation into heat sink.

# Installing Cells into Heat Sink

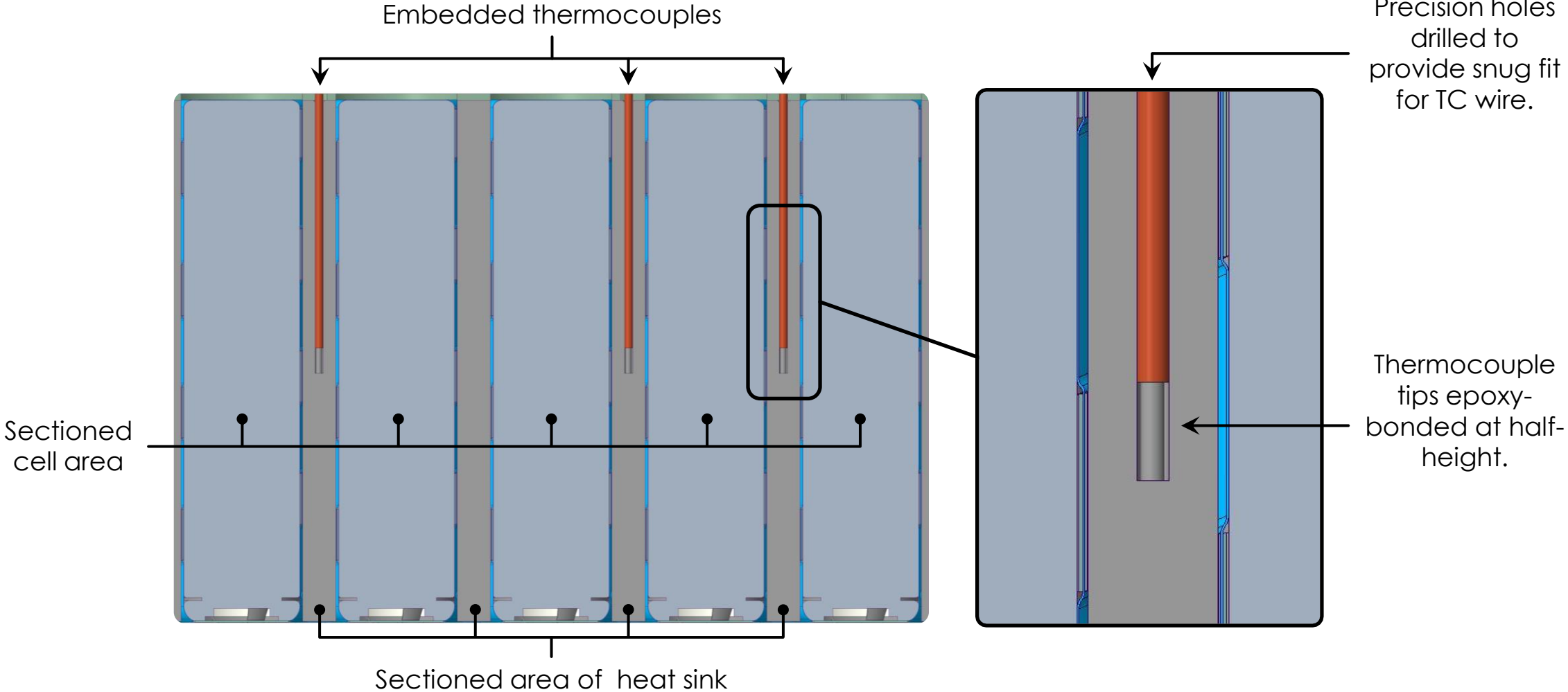


Epoxy adhesive is applied onto the cell followed by axial insertion into the heat sink (134 cells per virtual cell).



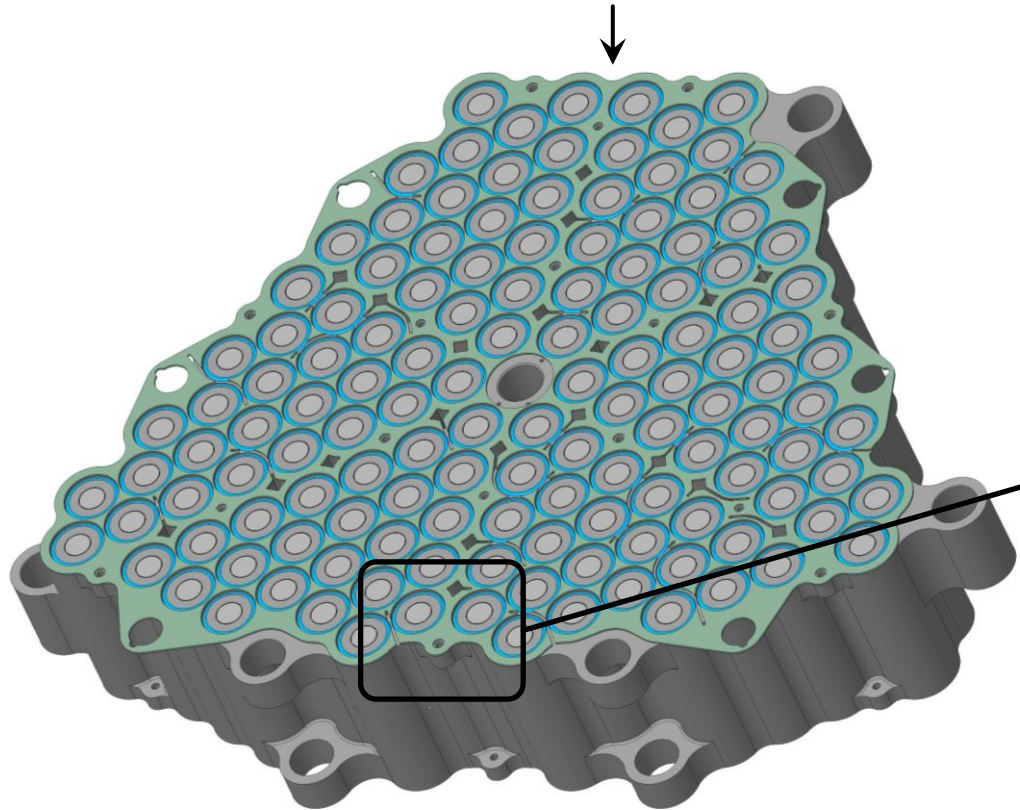
Thermocouples (TCs) installed in strategic locations (brown markers) to monitor the temperature of the heat sink during thermal runaway (Type K, 45 TCs in total, installed axially and radially).

# Thermocouple Installation

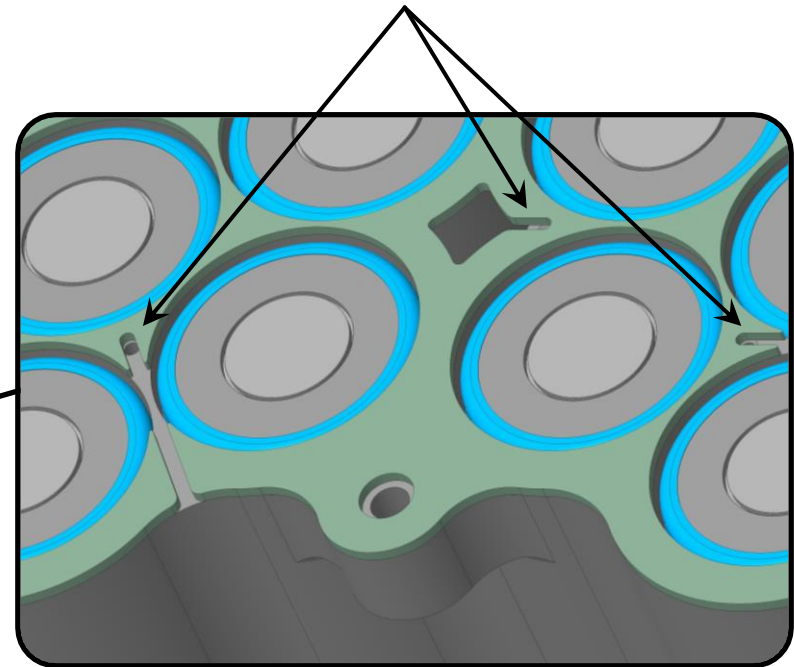


# Thermocouple Routing

Insulation plate bonded to heat sink via adhesive providing electrical insulation.

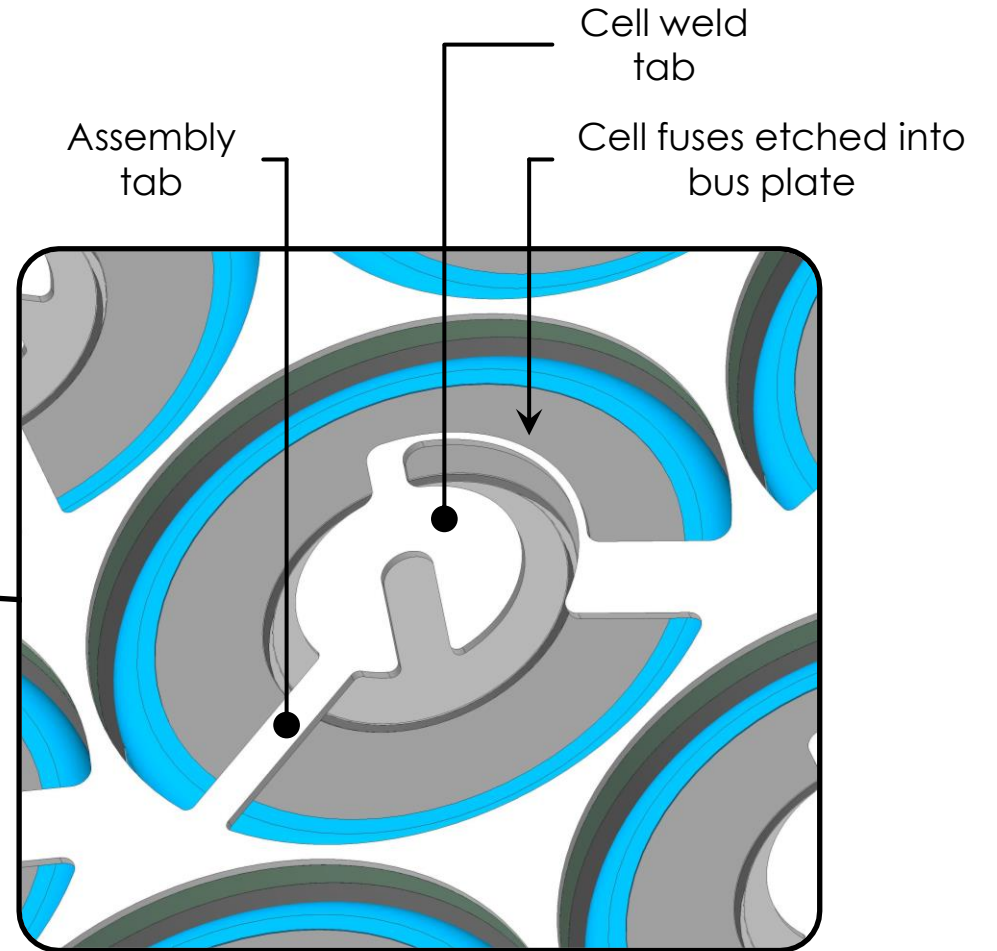
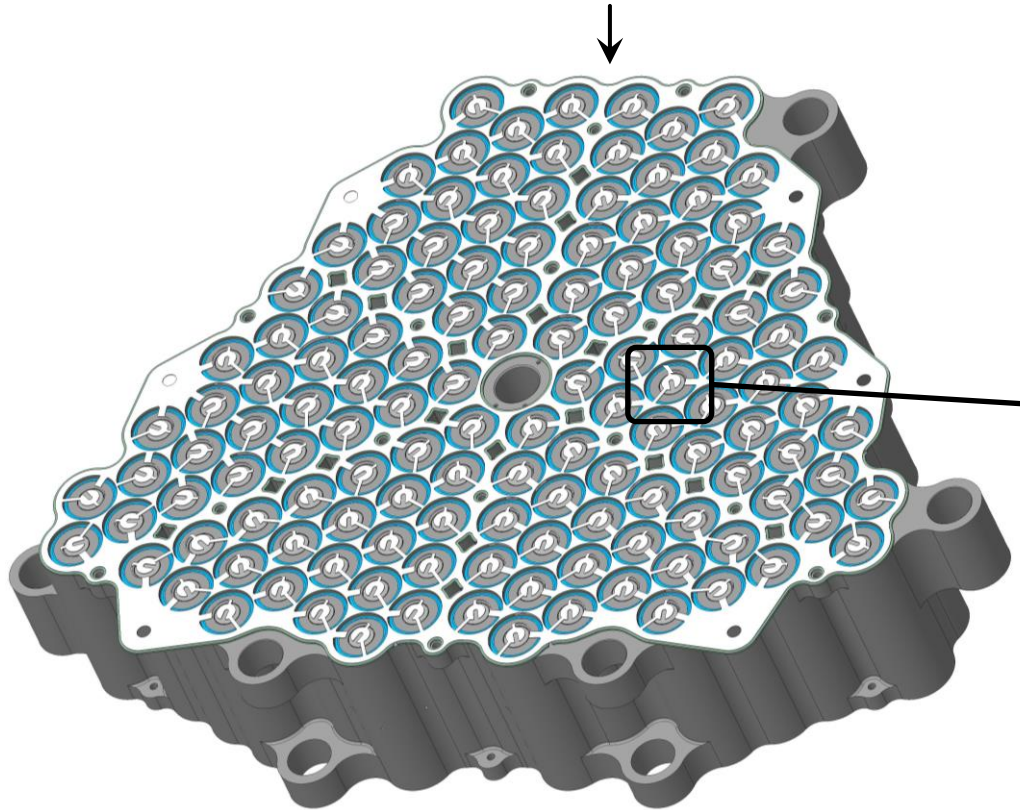


Grooves were machined into insulation plate to embed TCs to protect them from hot ejecta spray leaving cells during thermal runaway events.



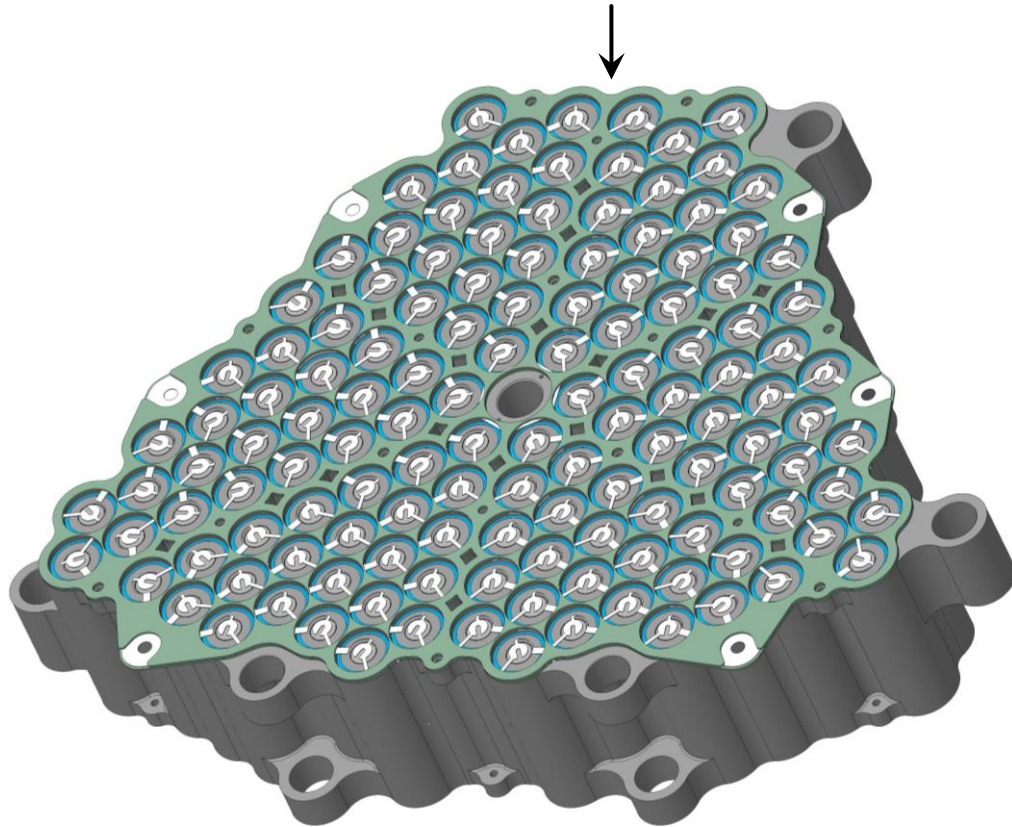
# Negative Bus Plate Assembly

Negative bus plate (nickel) epoxy-bonded to insulation plate. The bus plate provides a shielding layer for TR ejecta.

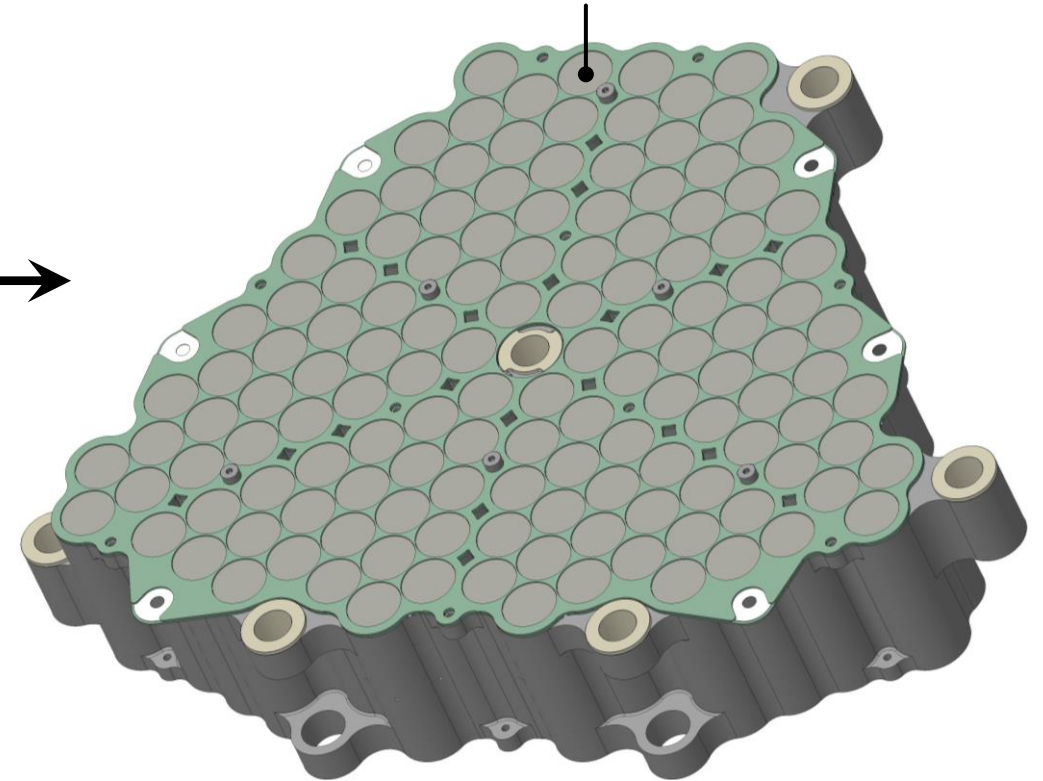


# Negative Bus Plate Assembly (cont.)

Upper layer of insulating material bonded to bus plate via epoxy and secured in place followed by welding and trimming of assembly tabs.

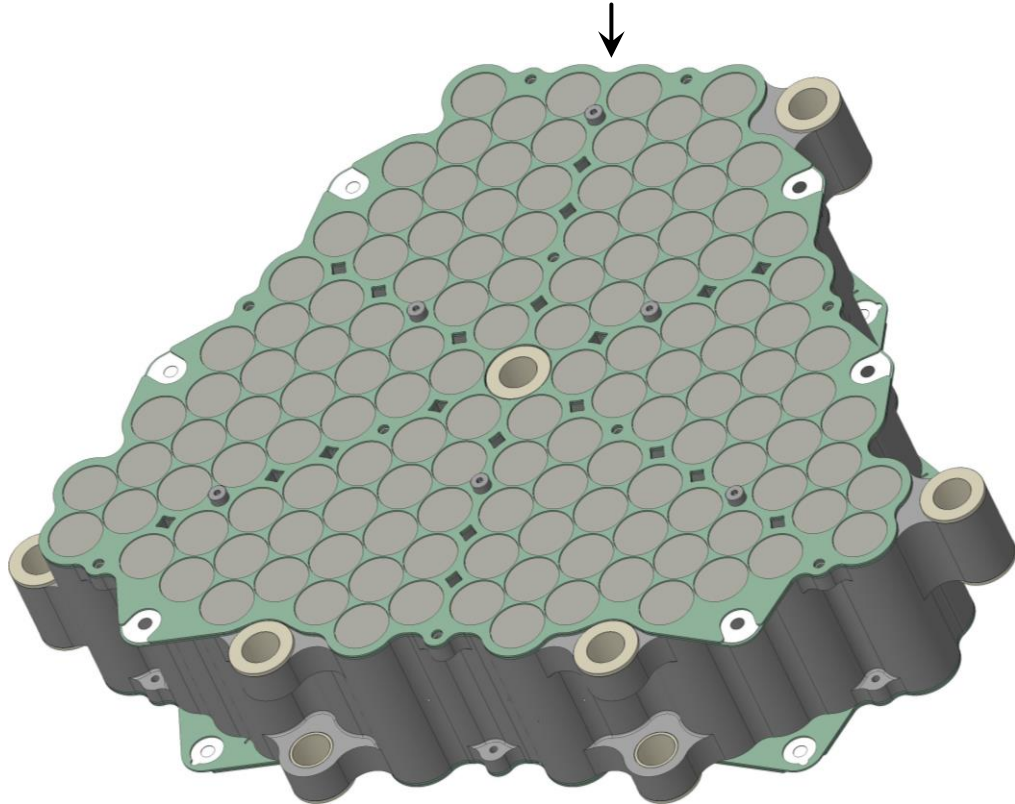


Circular mica covers placed into each cell to protect from TR ejecta, secured in place with two beads of epoxy. Electrically-insulating bushings installed into heat sink (x7).

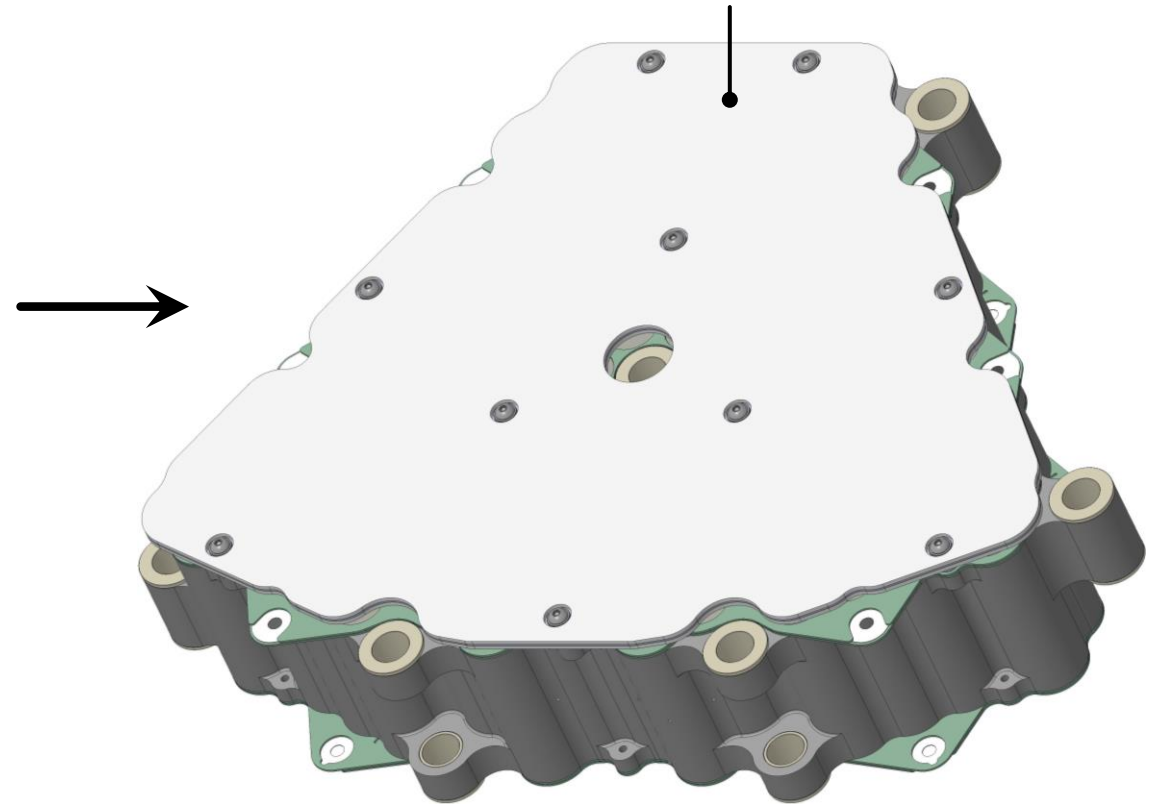


# Positive Bus and Blast Plates Assembly

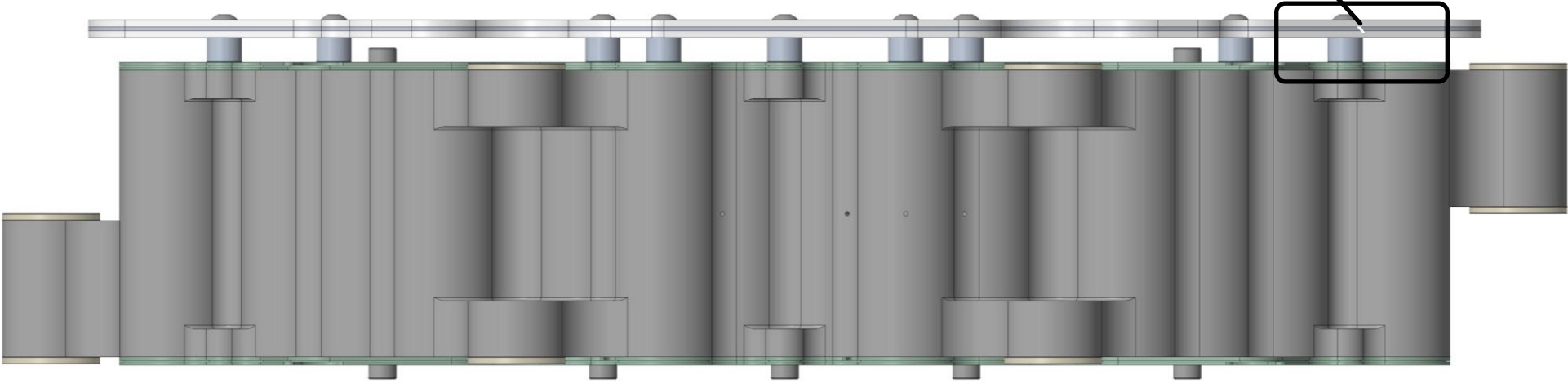
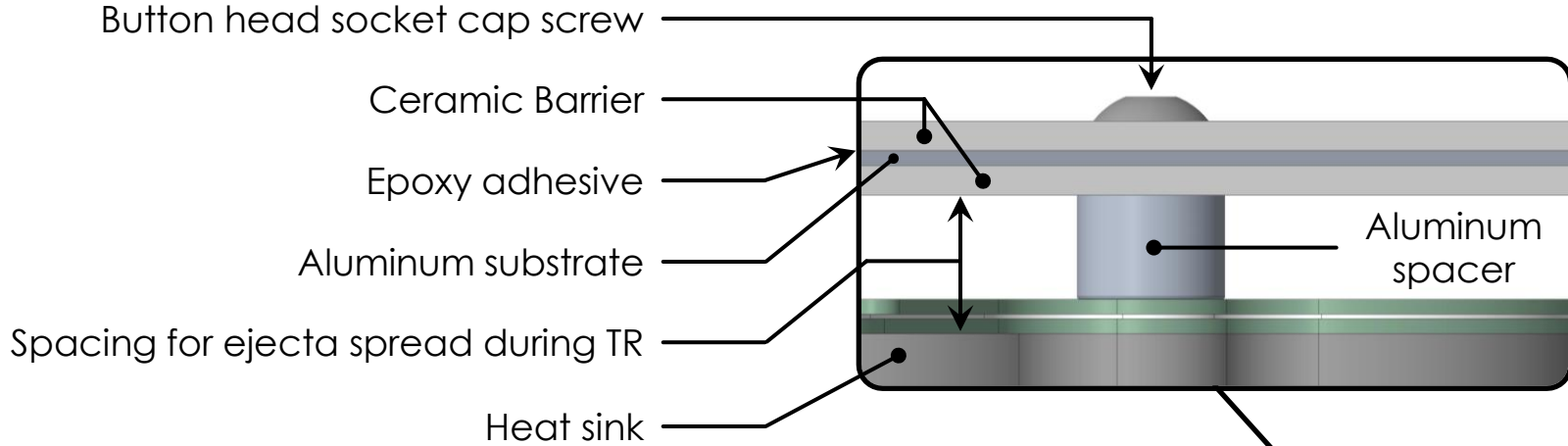
G10/Nickel/G10 sandwich bonded to positive side of virtual cell, bonding with epoxy between layers. Positive bus does not have cell fuses.



Ceramic reinforced aluminum blast plate assembled to heat sink, secured in at a controlled standoff distance of above cells. Complete **Virtual Cell Unit**.

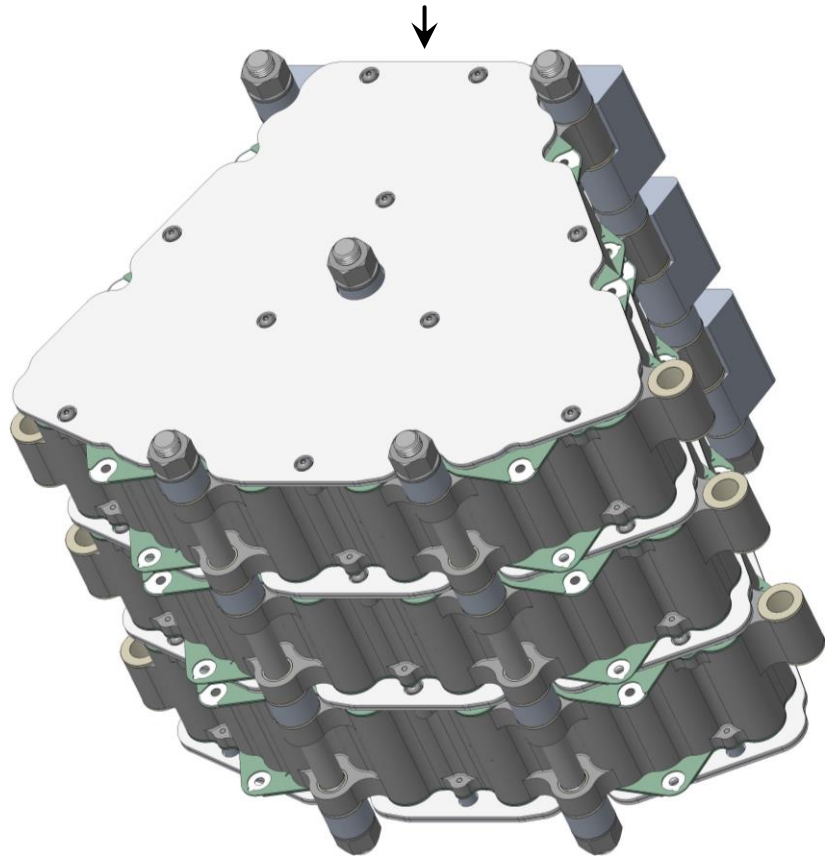


# Blast Plate Assembly Details

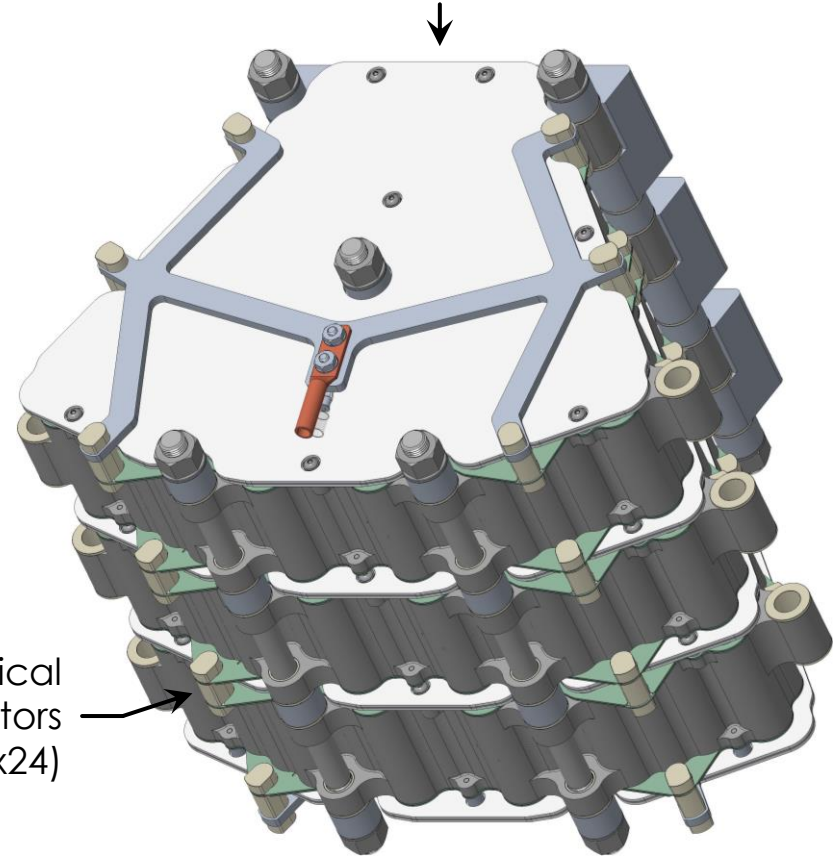


# Blast Plate Assembly Details

Virtual cells (x3) stacked axially, separated by aluminum spacers, connected mechanically with  $\frac{1}{2}$ -13 threaded rods (x5). Aluminum stability feet added for PPR testing.



Virtual cells connected electrically in series (3s) using aluminum standoffs (x6) and bused to single terminal via aluminum bus bars (positive and negative).



Electrical connectors (x24)

# Assembled PPR Test Article

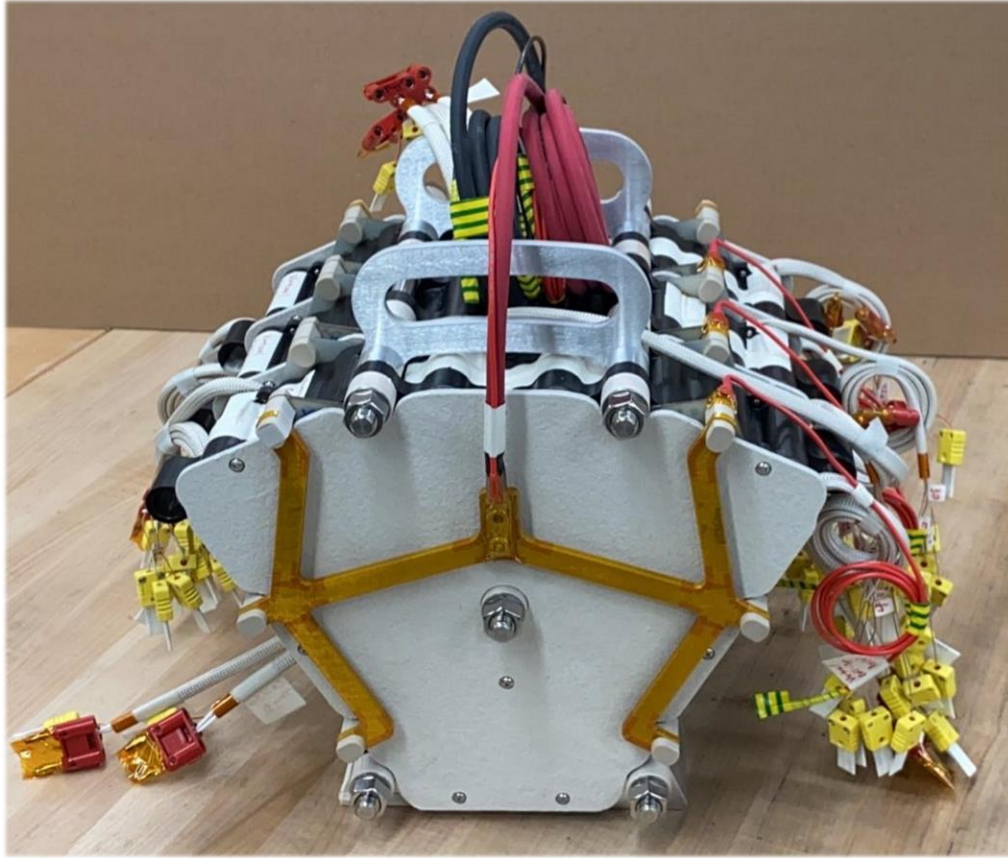


**Figure:** Front view of M3 PPR test article with trigger cell heaters, thermocouples, and voltage sense lines.

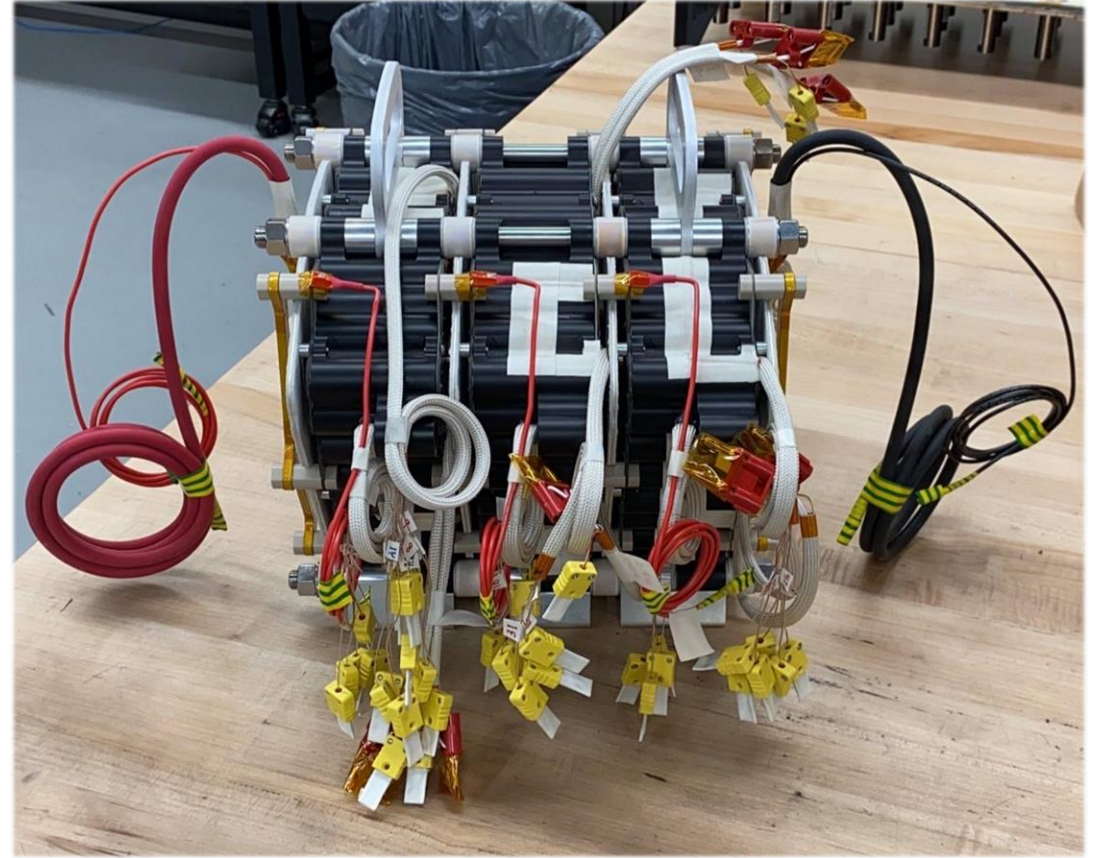


**Figure:** 60 thermocouples, 12 heating elements and 16 voltage sense lines installed onto M3 PPR Battery.

# NREL/NASA Cell Internal Short Circuit Device

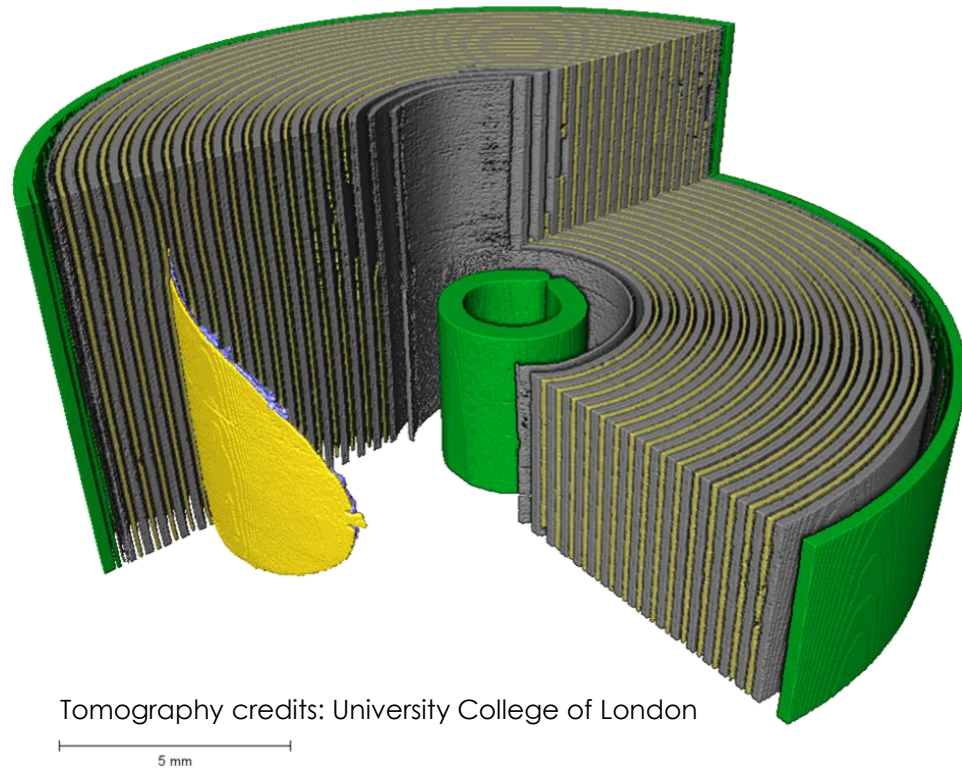


**Figure:** ISC Device in 2.4Ah cell design provides active anode to cathode collector short placed 6 winds into the jellyroll.

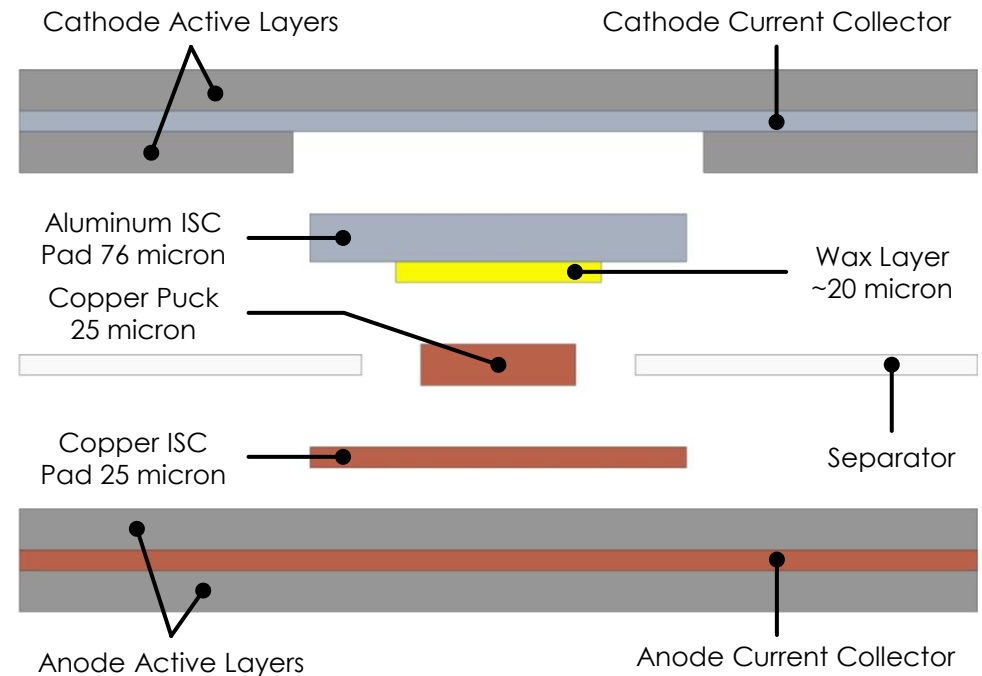
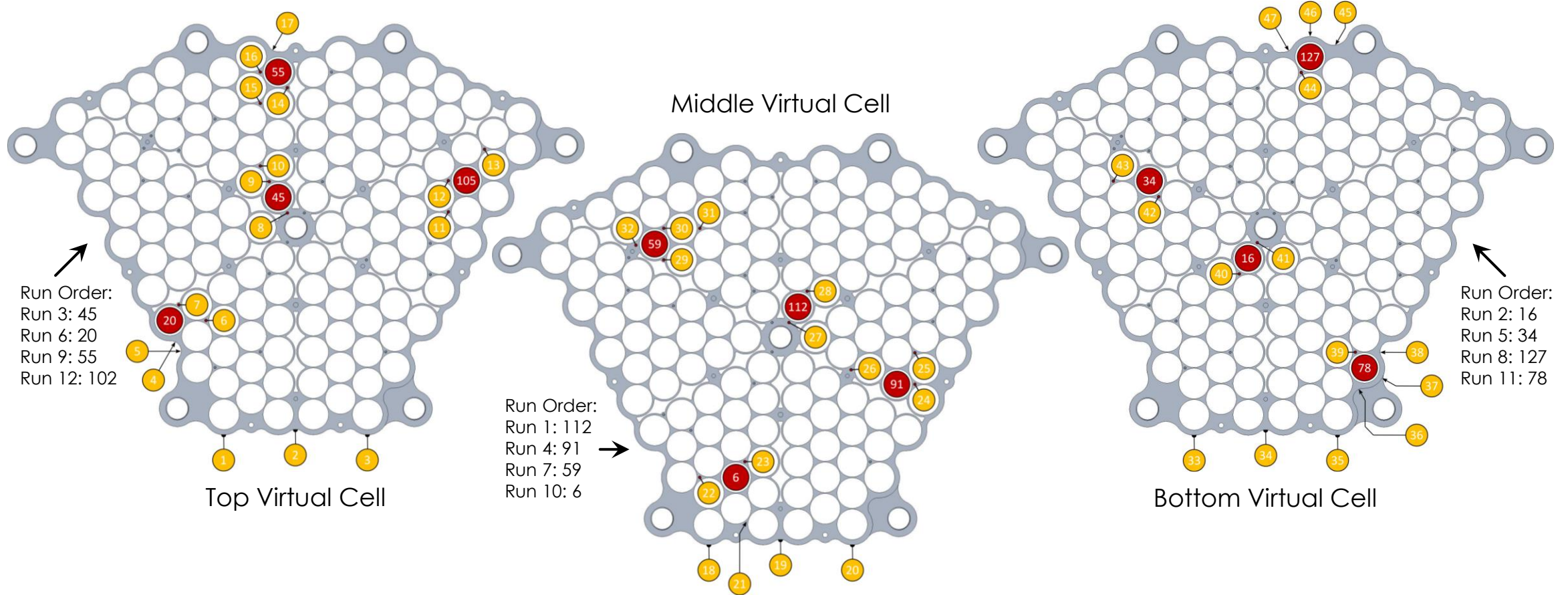


**Figure:** US Patent # 9,142,829 issued in 2015. Thin (10-20  $\mu\text{m}$ ) wax layer is spin coated onto aluminum foil, melting at  $57 \pm 5^\circ\text{C}$ , and creates an active short to initiate cell thermal runaway at a moderately low temperature.

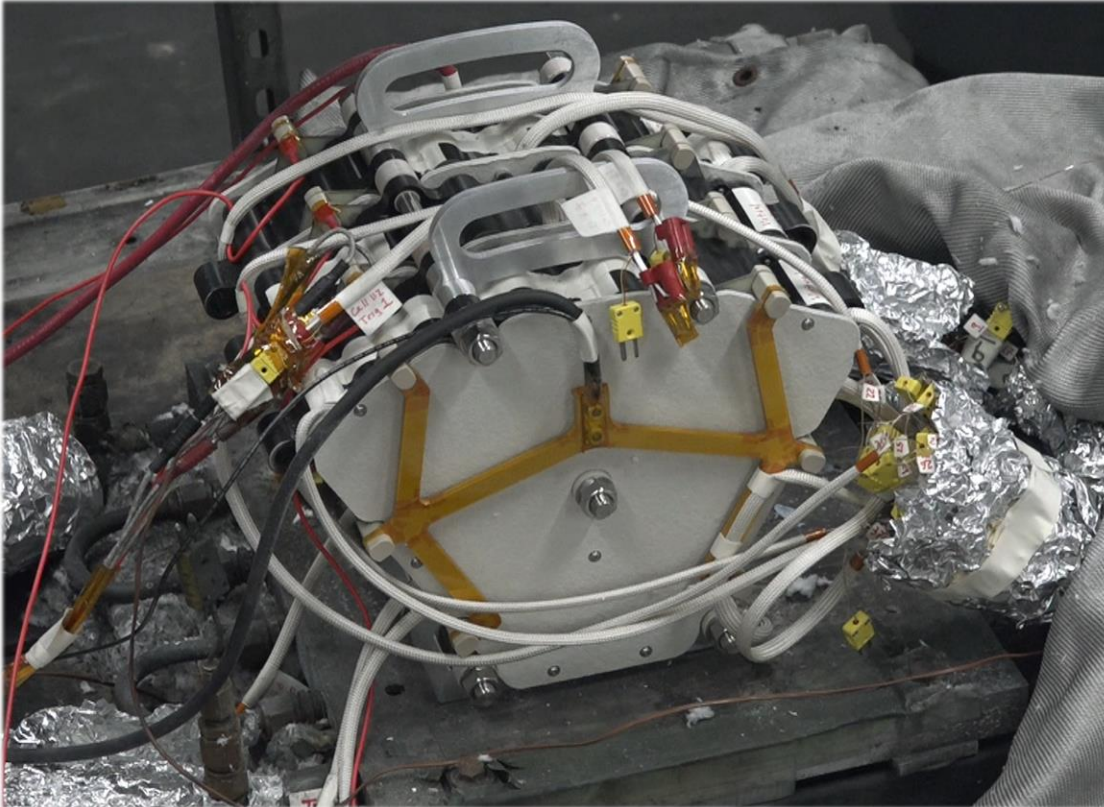
# Trigger Cell Locations and TC Map



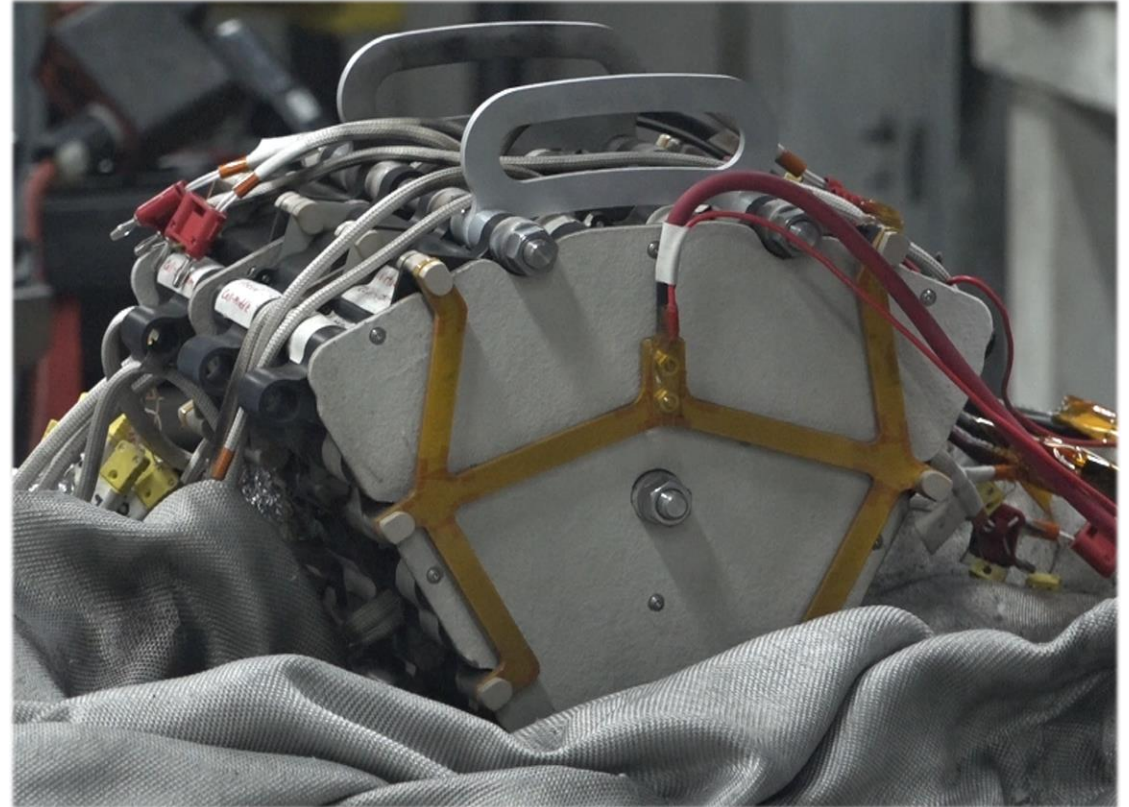
**Figures:** Molicel M35A trigger cells installed strategically (red circles), activated sequentially to simulate single-point cell failures. TC (yellow circles) measurements help to anchor thermal model. PPR Battery conditioned to 45 °C prior to each TR event.

# THERMAL RUNAWAY TEST RESULTS

# M3 Thermal Runaway Test Videos



**Video:** First M3 thermal runaway video (middle virtual cell, trigger cell located in the center).



**Video:** Last M3 thermal runaway video (virtual cell in "top/front" virtual cell, trigger cell in the upper middle).

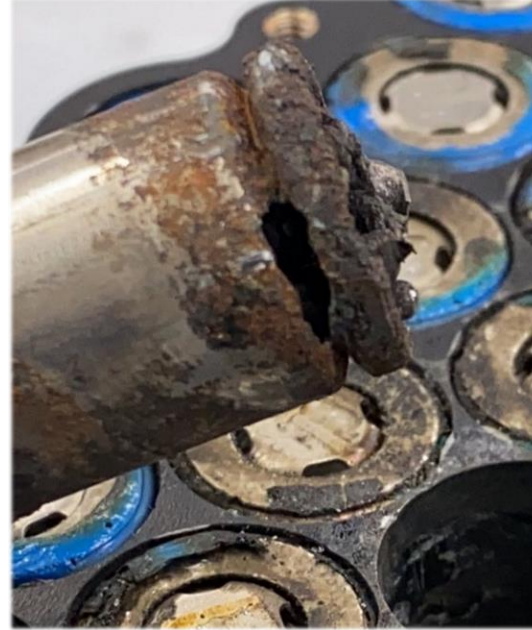
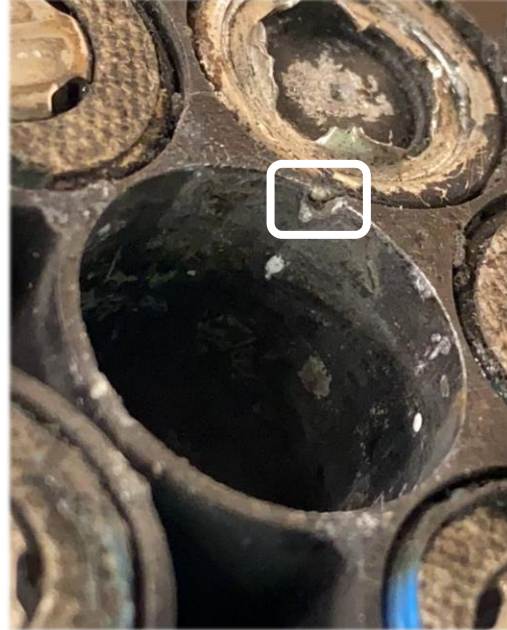
# Sample Cell Failure Mechanisms



**Run 1, Trigger Cell #112:** Cell experienced SWR, SGR and BR. Minor damage to bore anodization but no perforations in aluminum.

**Run 3, Trigger Cell #45:** Experienced SWR, SGR and BR. No bore damage observed.

# Sample Cell Failure Mechanisms (cont.)



**Run 4, Trigger Cell #91:** Large SWR and SGR observed on cell along with hole in aluminum bore. Lends explanation for shorted adjacent cell (0V cell).

**Run 5, Trigger Cell #34:** Large SGR, SWR and BR. No damage observed to bore.

# Sample Cell Failure Mechanisms



**Run 2, Trigger Cell #16:** Multiple SGRs, no visible damage to bore.



**Run 6, Trigger Cell #20:** Header assembly release, no SWR or SGR but had BR. No bore damage.

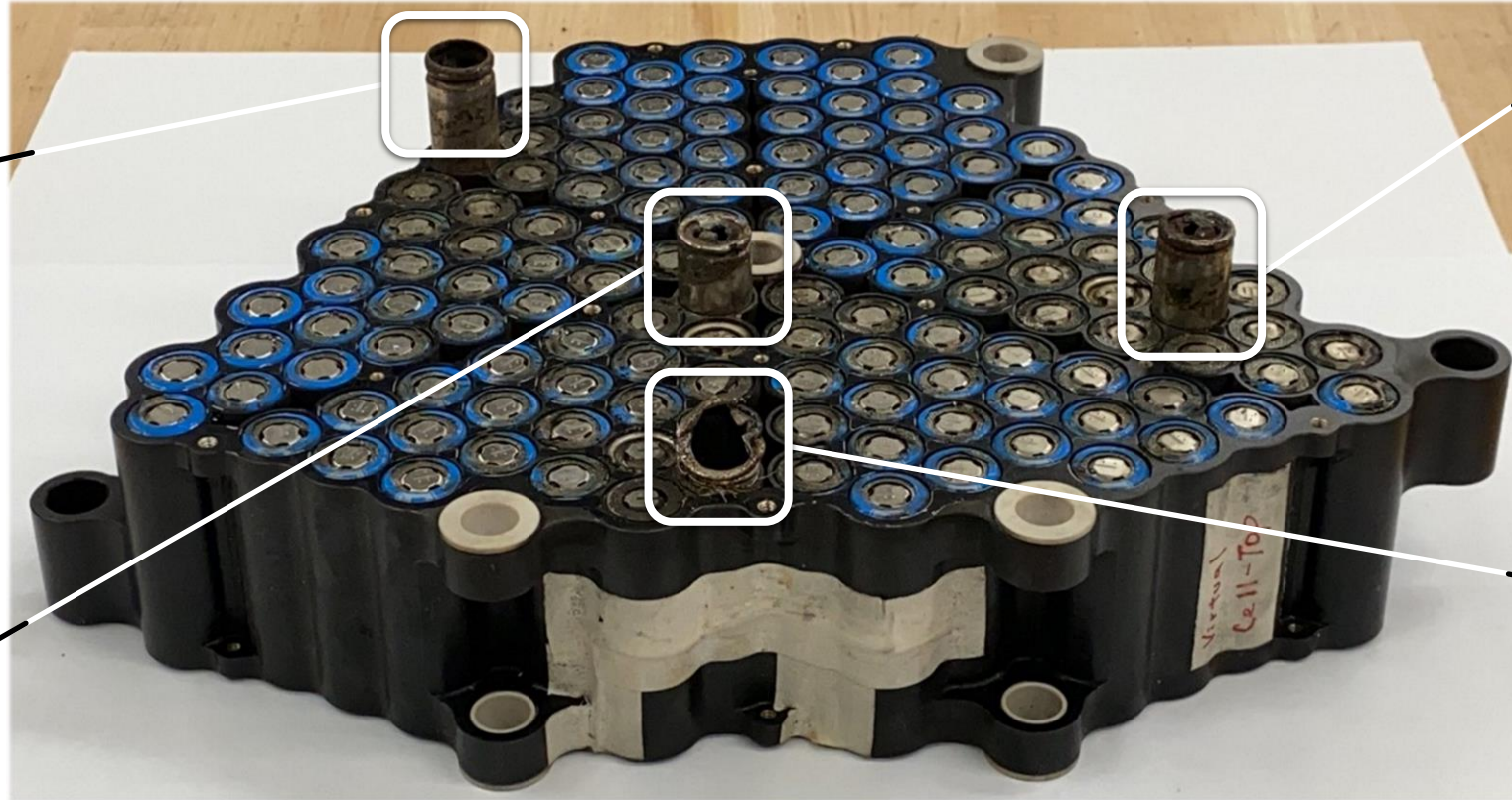


**Run 10, Trigger Cell #6:** Cell experienced SWR and BR but no SGR. No damage observed to bore. Header release occurred during TR.

# Post-Test DPA Results - Top Virtual Cell

Run 6 (Cell 20):  
Header assembly release, no SWR or SGR but had BR. No bore damage.

Run 3 (Cell 45):  
Experienced SWR, SGR and BR. No bore damage observed.



Run 12 (Cell 105):  
Tiny SGR, BR, no bore damage.

Run 9 (Cell 55):  
Cell damaged during first extraction trial. No BR, slight anodize damage (possibly during extraction).

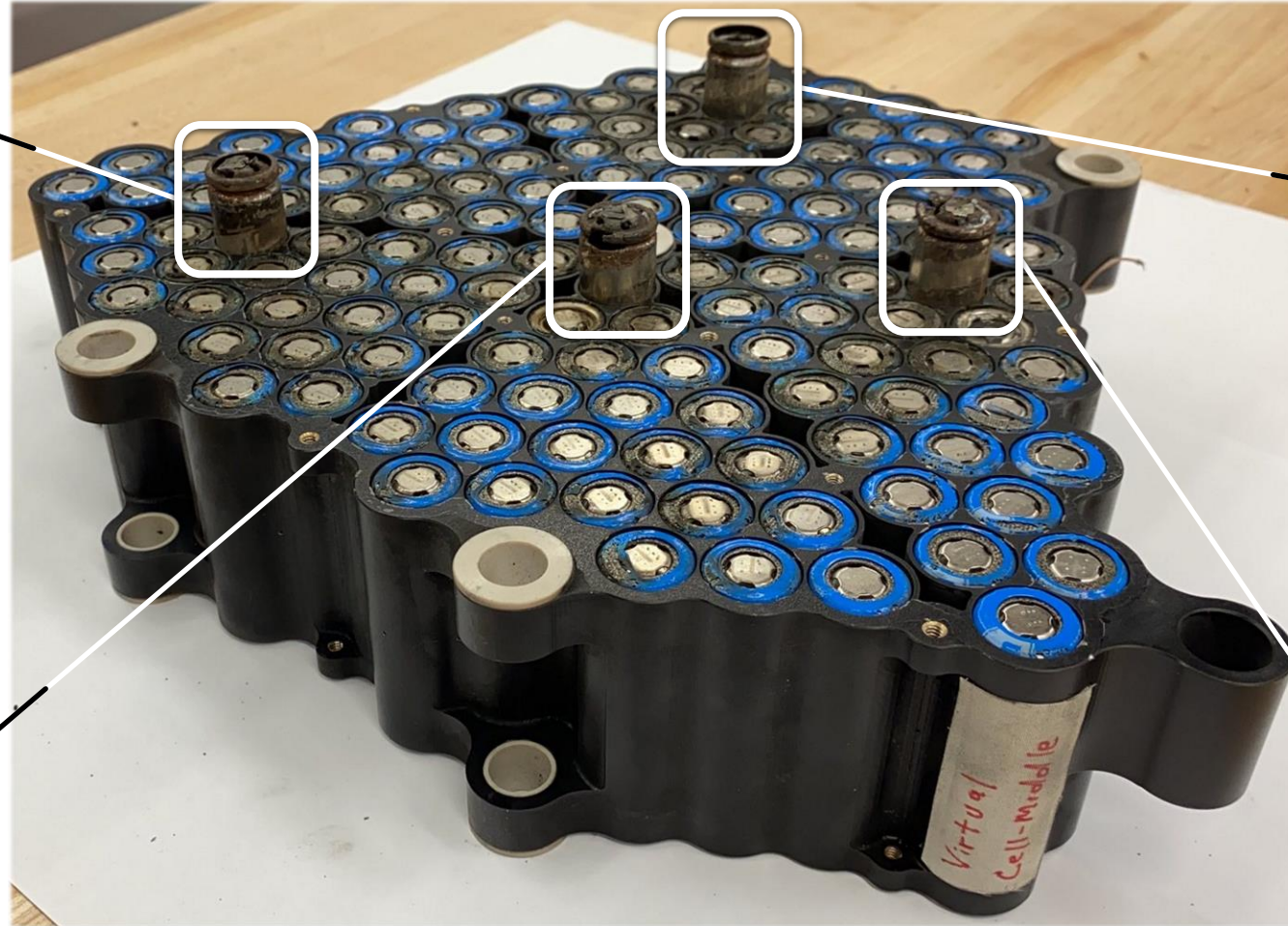
# Post-Test DPA Results - Middle Virtual Cell

## Run 7 (Cell 59):

No SWR or SGR, but cell experienced BR. No damage to the bore observed.

## Run 1 (Cell 112):

Cell experienced SWR, SGR and BR. Minor damage to bore anodization but no perforations in aluminum.



## Run 10 (Cell 6):

Cell experienced SWR and BR but no SGR. No damage observed to bore. Header release occurred during TR.

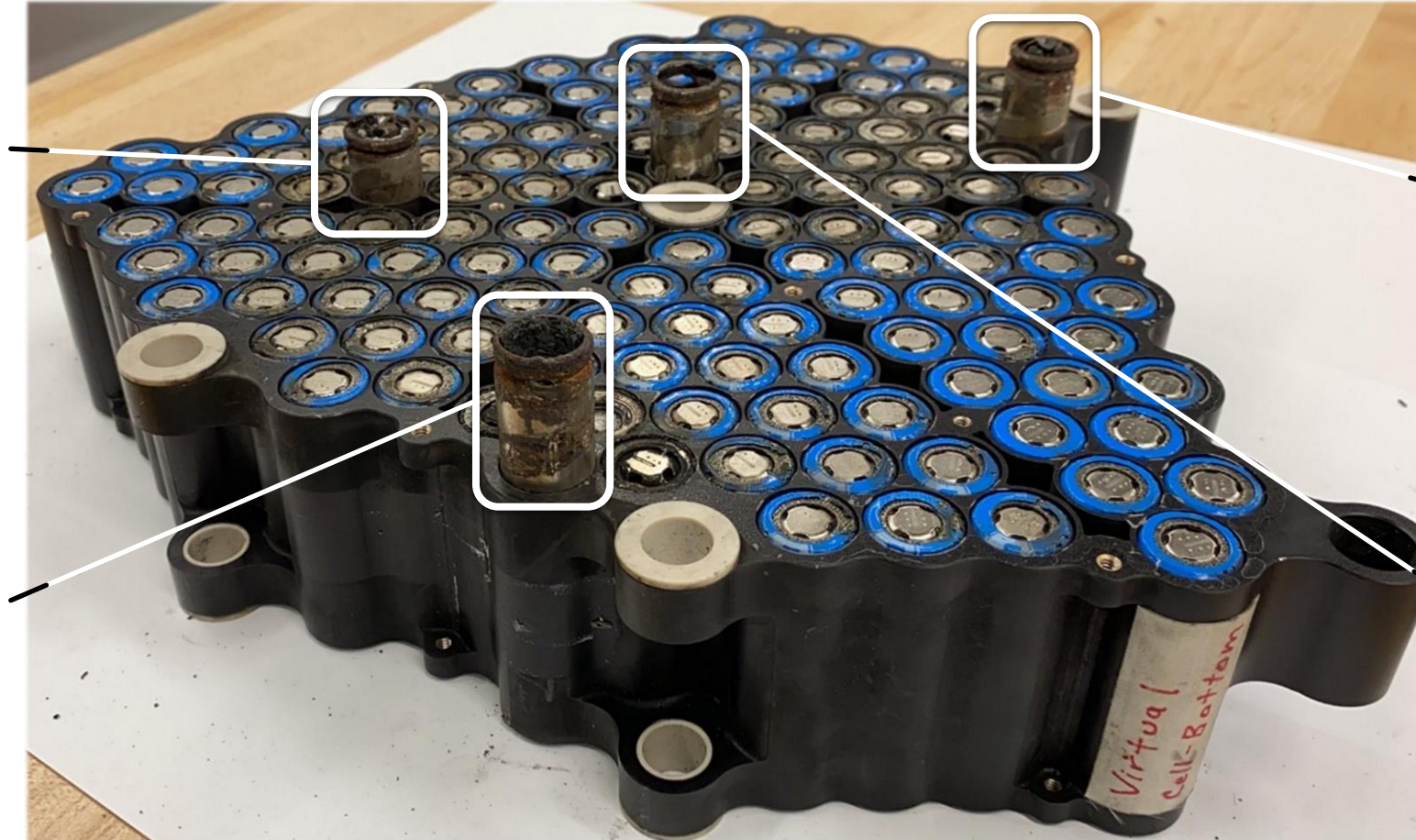
## Run 4 (Cell 91):

Large SWR and SGR observed on cell along with hole in aluminum bore. Lends explanation for shorted adjacent cell (0V cell).

# Post-Test DPA Results - Bottom Virtual Cell

Run 5 (Cell 34):  
Large SGR, SWR  
and BR. No  
damage  
observed to  
bore.

Run 8 (Cell 127):  
Cell header  
release and BR.  
No SWR, SGR or  
damaged to  
bore observed.



Run 11 (Cell 78):  
Cell experienced  
SGR and BR. No  
damaged  
observed to  
bore.

Run 2 (Cell 16):  
Multiple SGRs,  
no visible damage  
to bore.

# Summary of Trigger Cell Events

Run Number	Virtual Cell	Trigger Location	Cell Position	Bottom Rupture	SWR, SGR?	Bore Damage	Blown Adjacent Cell Fuses
1	Middle	Center, 2 Adj. Cells	112	Yes	SWR, SGR	No	No
2	Bottom	Center, 2 Adj. Cells	16	No	SGRs	No	No
3	Top	Center, 2 Adj. Cells	45	Yes	SWR, SGR	No	No
10	Middle	Interior, 6 Adj. Cells	6	Yes	No	No	Yes, Cell 22, 0V
11	Bottom	Edge, 3 Adj. Cells	78	No	SGR	No	Yes, Cell 74, 0V
6	Top	Edge, 2 Adj. Cells	20	Yes	No	No	No
Overnight	Bottom	Edge, 3 Adj. Cells	78	Run 11	Activated	-	-
5	Bottom	Interior, 4 Adj. Cells	34	Yes	SGR, SWR	No	No
8	Bottom	Edge, 3 Adj. Cells	127	Yes	No	No	Yes, Cell 44, 0V
4	Middle	Interior, 4 Adj. Cells	91	Yes	SWR, SGR	Burn Through	Yes, Cell 25, 0V
7	Middle	Interior, 4 Adj. Cells	59	Yes	No	No	Yes, Cell 29, 3.55V
12	Top	Interior, 6 Adj Cells	105	Yes	Tiny SGR	No	No
9	Top	Edge, 3 Adj. Cells	55	No	No	No	No

# DPA Findings and Conclusions

- All ISCD Trigger Cells activated without TR propagation. Blast plates protected axially stacked virtual cells well
  - Post PPR battery stack discharge capacity of 401 Ah
  - Top Virtual Cell:
    - Three (3) cells experienced BR, no blown fuses on adjacent cells
    - 2% degradation vs 3.5Ah/cell (post-test average: 3.42Ah/cell)
  - Middle Virtual Cell:
    - Four (4) trigger cells experienced BR, three (3) blown fuses on adjacent cells
    - 4% degradation vs 3.5Ah/cell (post-test average: 3.37Ah/cell)
  - Bottom Virtual Cell:
    - Three (3) trigger cells experienced BR, two (2) blown fuses on adjacent cells
    - 3% degradation vs 3.5Ah/cell (post-test average: 3.37Ah/cell)
- Design has robustly demonstrated PPR

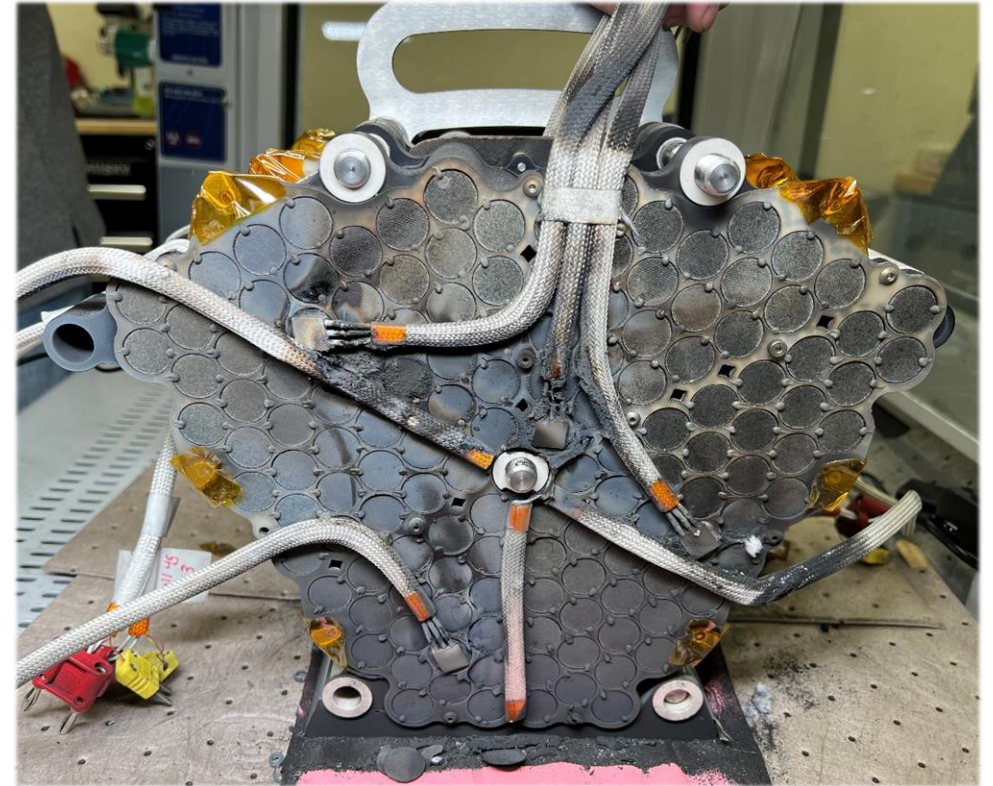
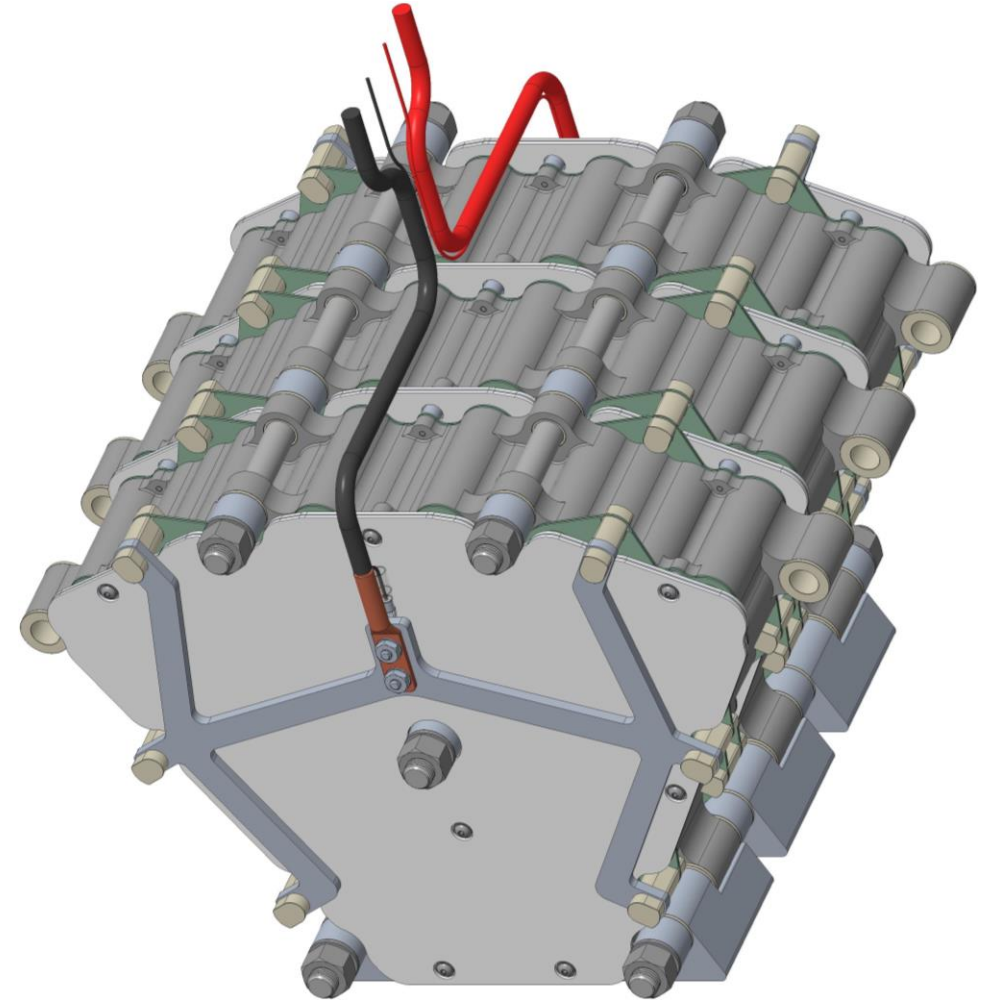


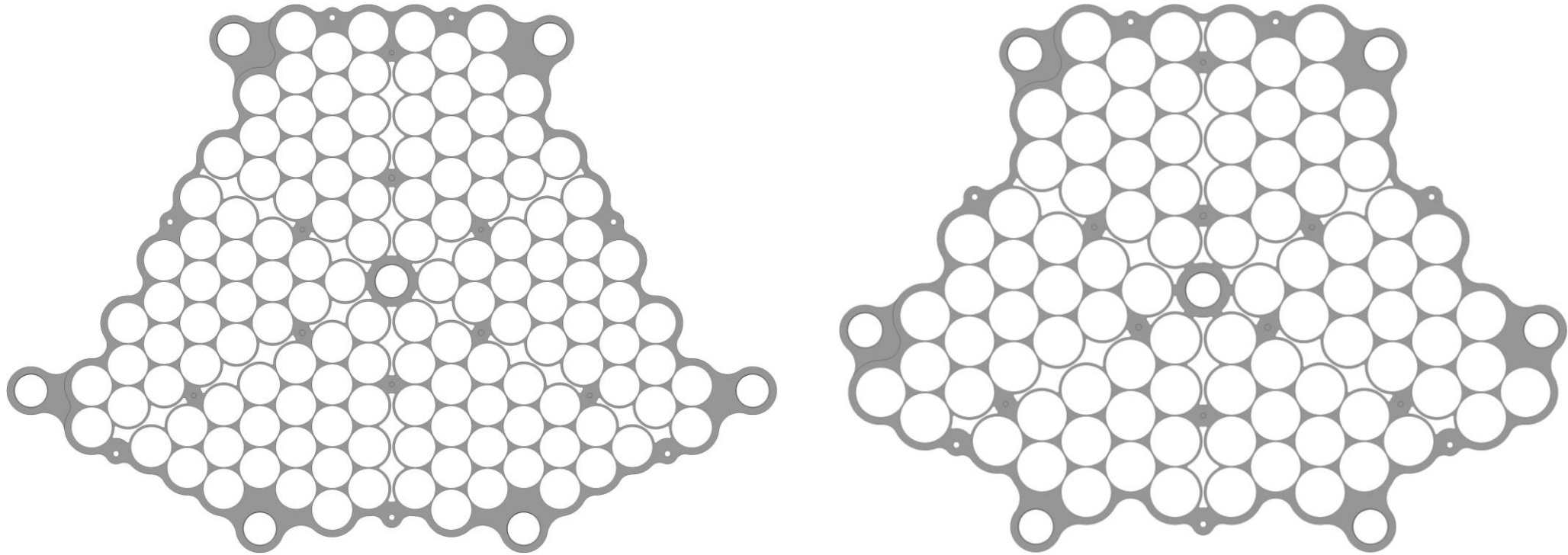
**Figure:** Negative side of middle virtual cell following post-test disassembly.

# M3 Battery Design Metrics

- PPR battery unit energy: **4.8 kWh**
  - 134P – 3S electrical topology
  - 390 Samsung M35A 18650 cells in total (12 Samsung M35A trigger cells)
- PPR Battery overall mass: **28.84 kg** [63.59 lbs]
- PPR Battery calculated energy densities:
  - Specific energy density: **166.44 Wh/kg**
  - Volumetric energy density: **459.39 Wh/L**
- PPR Battery calculated mass factors:
  - Percent cell mass versus total battery mass: **66.9%**
  - Parasitic mass factor: **1.495**
- PPR Battery miscellaneous metrics:
  - Mass percentage of heat sinks: **20.46%**
  - Mass percentage of blast plates: **1.60%**



# Development of 21700-Cell PPR Battery

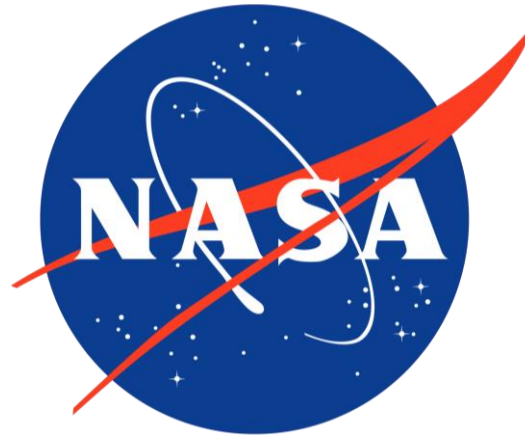


- Achieve PPR battery pack using 21700 cells leveraging lessons learned from 18650 PPR battery designs
- Provide direct comparison of 18650 M3 battery to 21700 M5 battery with modeling and test results to determine benefits and drawbacks of using 21700 cells in PPR packs compared to 18650 cells

# Acknowledgement of Partnership



Joe H. Fontaine (NSWC Crane, IN)  
John R. Izzo (NUWC Newport, RI)  
Thomas E. Adams (NSWC Crane, IN)  
Jacob L. Moyar



Eric C. Darcy (JSC)  
David Petrushenko (JSC)  
(John) Jacob Darst (JSC)  
Jesus Trillo



Ralph E. White  
Paul T. Coman  
David Petrushenko

The partnership between the NAVSEA, NASA Johnson Space Center and the University of South Carolina made this productive project possible. We acknowledge and appreciate all the contributions to this project!

THANK YOU!